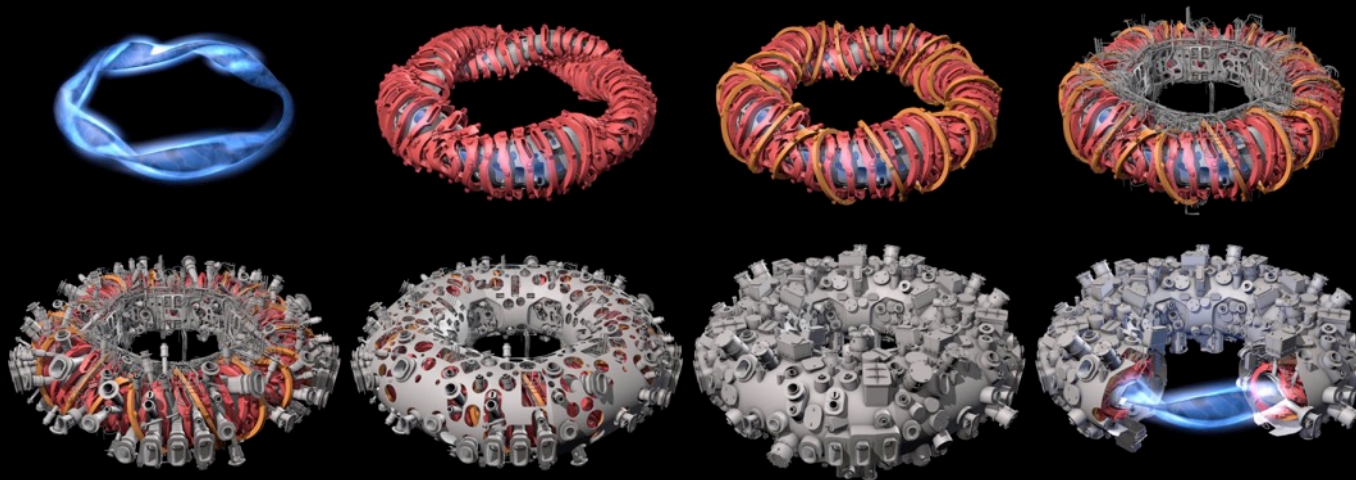


INVESTIGATIONS OF THE ROLE OF NEOCLASSICAL TRANSPORT IN ION-ROOT PLASMAS ON W7-X

NOVIMIR PABLANT ON BEHALF OF THE W7-X TEAM



MANY THANKS TO THE WHOLE WENDELSTEIN 7-X TEAM

Special thanks to my co-authors:

A. Langenberg, A. Alonso, J. Baldzuhn, C.D. Beidler, L.G. Böttger, S. Bozhenkov, K.J. Brunner, R. Burhenn, A. Dinklage, E. Edlund, G. Fuchert, O. Ford, D.A. Gates, J. Geiger, O. Grulke, M. Hirsch, U. Hoefel, Z. Huang, Y. Kazakov, J. Knauer, J. Kring, H. Laqua, M. Landreman, S. Lazerson, H. Massberg, O. Marchuck, A. Mollen, E. Pasch, A. Pavone, M. Porkolab, S. Satake, T. Schroeder, J. Svensson, P. Traverso, Y. Turkin, J.L. Velasco, A. Von Stechow, F. Warmer, G. Weir, R.C. Wolf, D. Zhang and the W7-X Team



THE FIRST OPERATIONAL PHASE OF WENDELSTEIN 7-X CONCLUDED ON OCTOBER 18, 2018

W7-X is the worlds first large scale optimized stellarator.

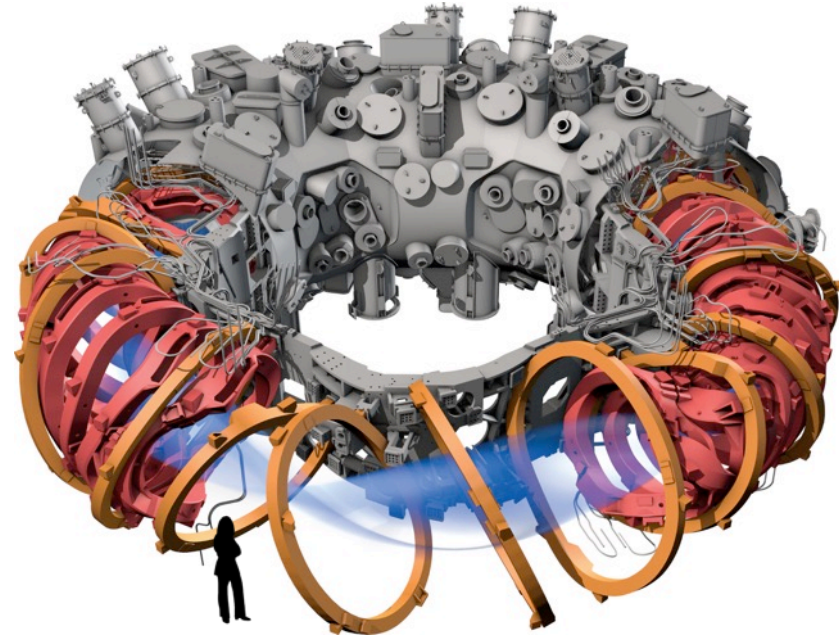
The plasma shape and coil set have been optimized to reduce neoclassical transport.
(along with other optimizations)

Expected operating scenario:

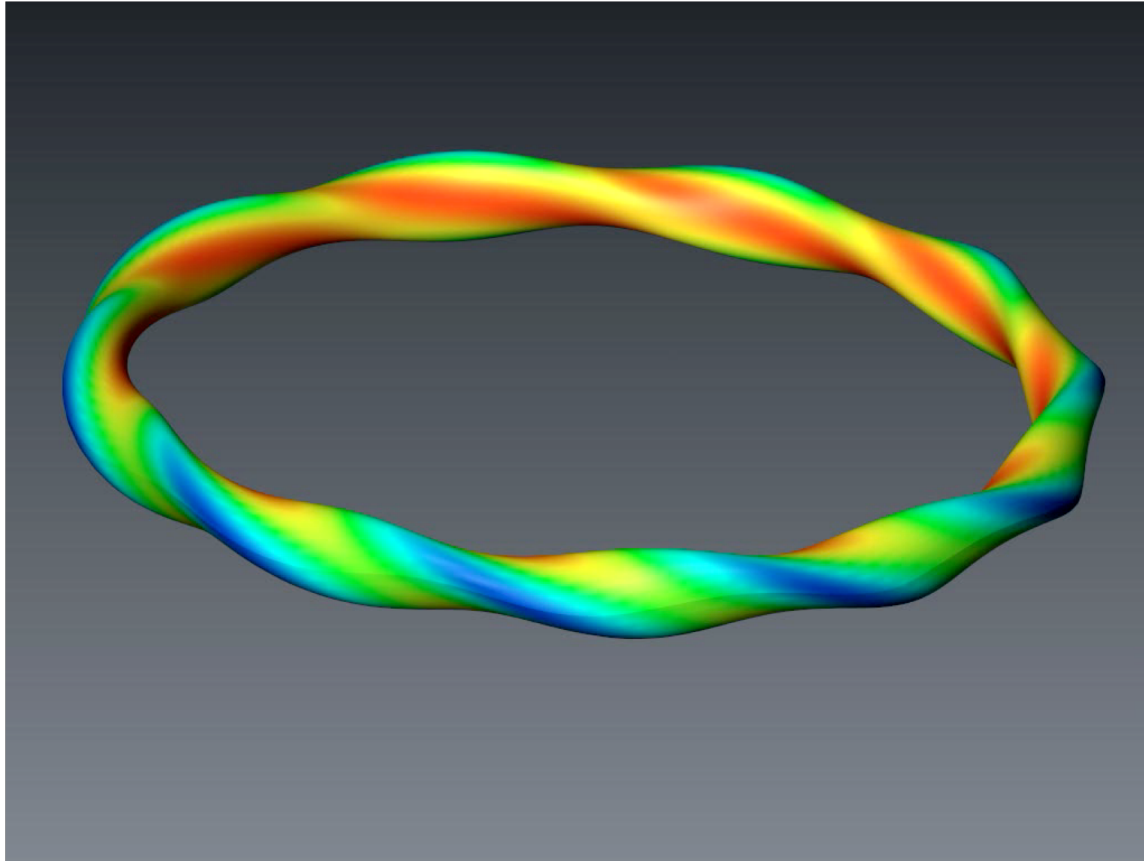
- High density ($2 \times 10^{20} \text{ m}^{-3}$)
- Electron heating with ECRH
- **Negative radial electric field (ion-root)**
- Volume averaged beta $\sim 5\%$

First operation phase of W7-X featured:

- Up to 7.0 MW of ECRH power
- Uncooled graphite island divertor
- 200 MJ injected power



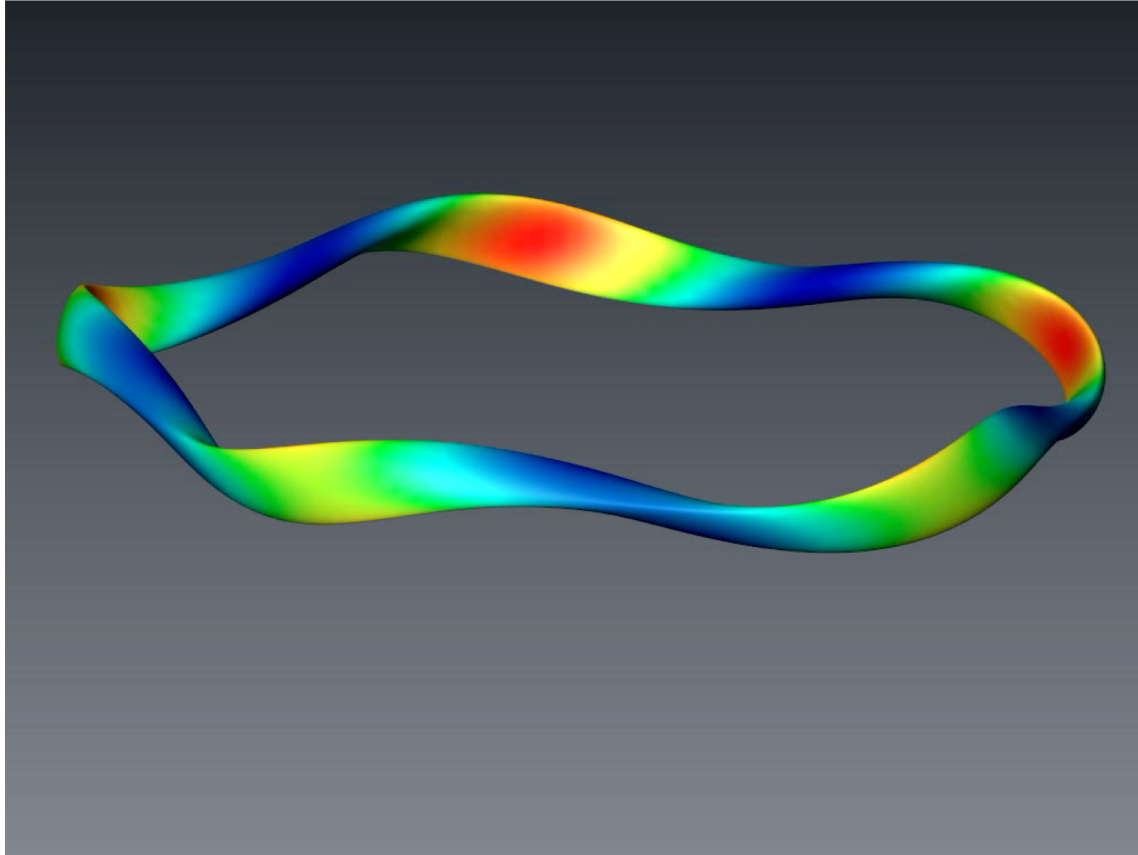
IN A CLASSICAL STELLARATOR TRAPPED PARTICLES ARE NOT WELL CONFINED AND DRIFT ACROSS FLUX SURFACES



Shown is the orbit of a 50 keV ion in a *classical* stellarator of similar size to W7-X.

This energy scales to an α -particle in a reactor scale device.

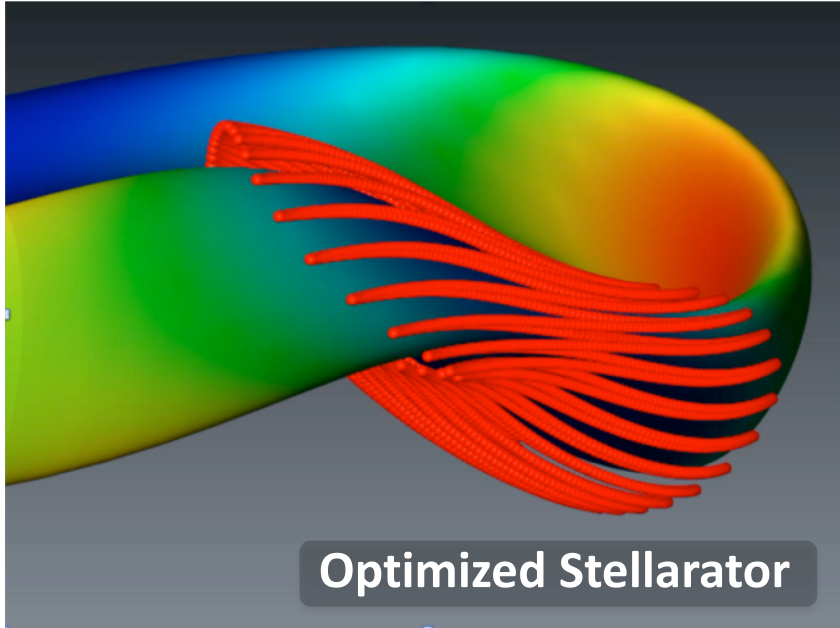
OPTIMIZATION OF THE MAGNETIC FIELD CAN PROVIDE GOOD CONFINEMENT OF BOTH PASSING AND TRAPPED PARTICLES



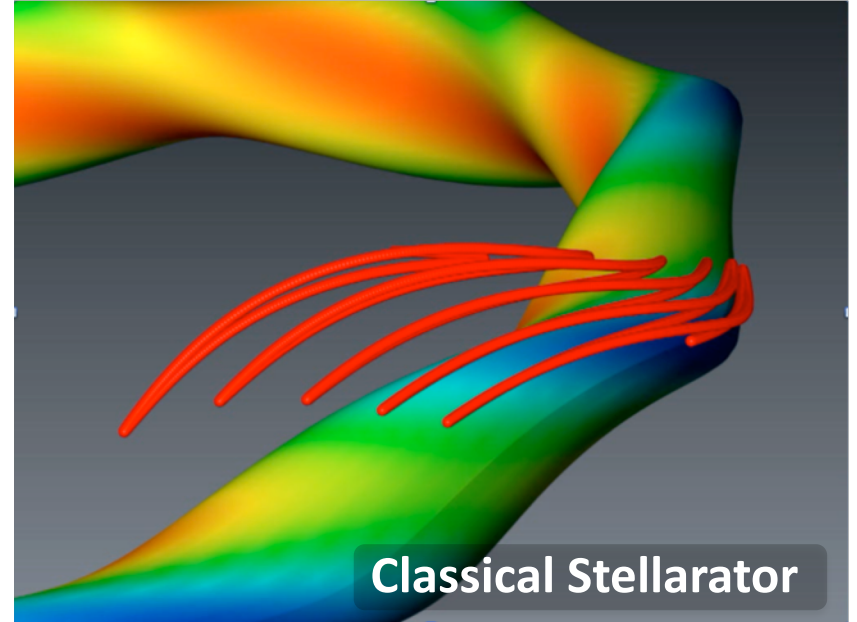
Shown is the orbit of a 50 keV ion in an optimized stellarator of similar size and design as W7-X.

This energy scales to an α -particle in a reactor scale device.

OPTIMIZATION OF THE MAGNETIC FIELD CAN PROVIDE GOOD CONFINEMENT OF BOTH PASSING AND TRAPPED PARTICLES



Shown is the orbit of a 50 keV ion in an optimized stellarator of similar size and design as W7-X.



This energy scales to an α -particle in a reactor scale device.

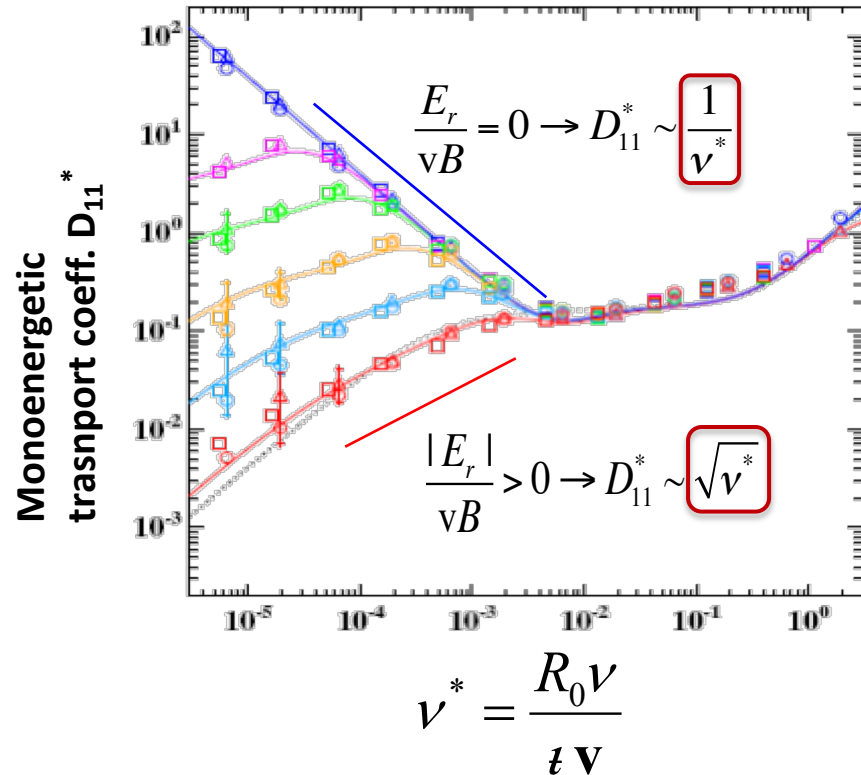
IN STELLARATORS TRANSPORT IS STRONGLY DEPENDENT ON THE RADIAL ELECTRIC FIELD

At low collisionalities the radial electric field is expected to substantially affect neoclassical heat and particle transport.

This is different than in tokamaks.

For a tokamak:

- Particle fluxes are intrinsically ambipolar.
- Particle fluxes and neoclassical transport are independent of E_r .



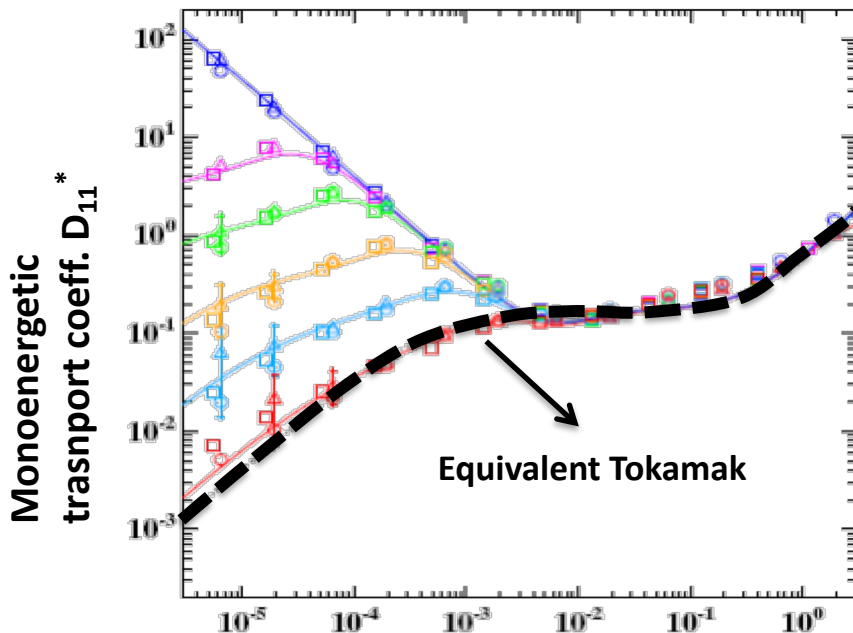
IN STELLARATORS TRANSPORT IS STRONGLY DEPENDENT ON THE RADIAL ELECTRIC FIELD

At low collisionalities a large positive E_r is expected to substantially reduce neoclassical heat transport.

This is different than in tokamaks.

For a tokamak:

- Particle fluxes are intrinsically ambipolar.
- Particle fluxes and neoclassical transport are independent of E_r .



$$\nu^* = \frac{R_0 v}{\ell v}$$

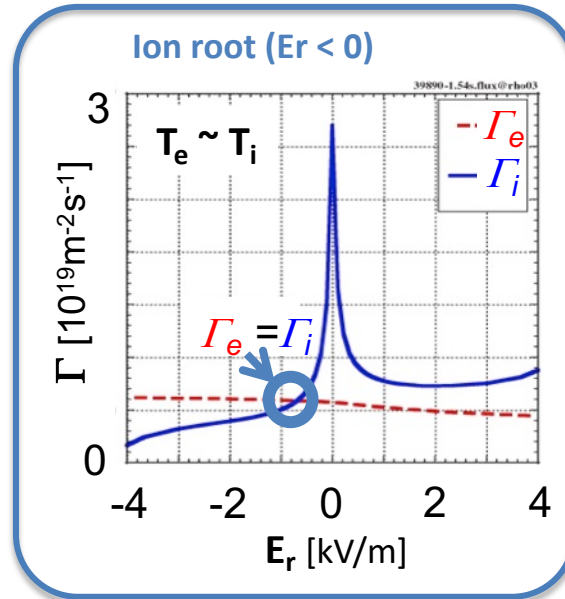
IN STELLARATORS THE RADIAL ELECTRIC FIELD PLAYS A SPECIAL ROLE IN PLASMA CONFINEMENT

Neoclassical ion and electron particle fluxes are affected by the radial electric field.

- Local ambipolarity is only consistent with particular values of E_r .

At high densities with $T_e \sim T_i$ there is typically a single solution for E_r :

- ion root ($E_r < 0$)



IN STELLARATORS THE RADIAL ELECTRIC FIELD PLAYS A SPECIAL ROLE IN PLASMA CONFINEMENT

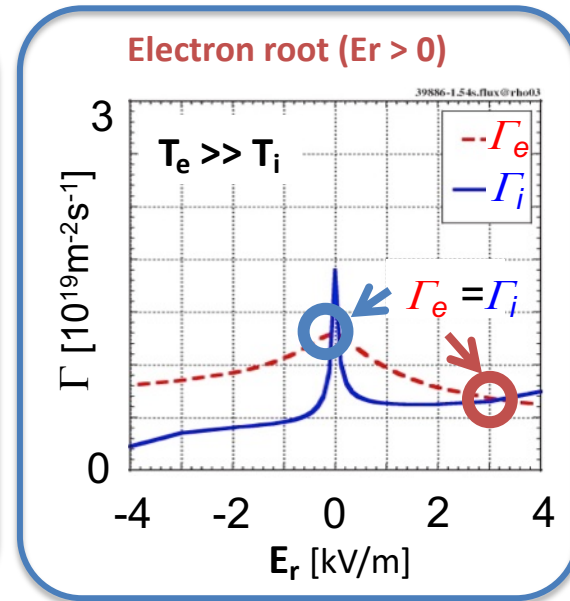
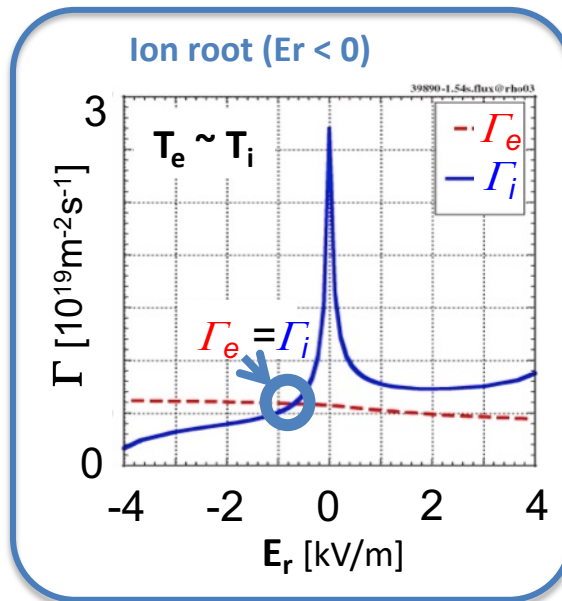
Neoclassical ion and electron particle fluxes are affected by the radial electric field.

- Local ambipolarity is only consistent with particular values of E_r .

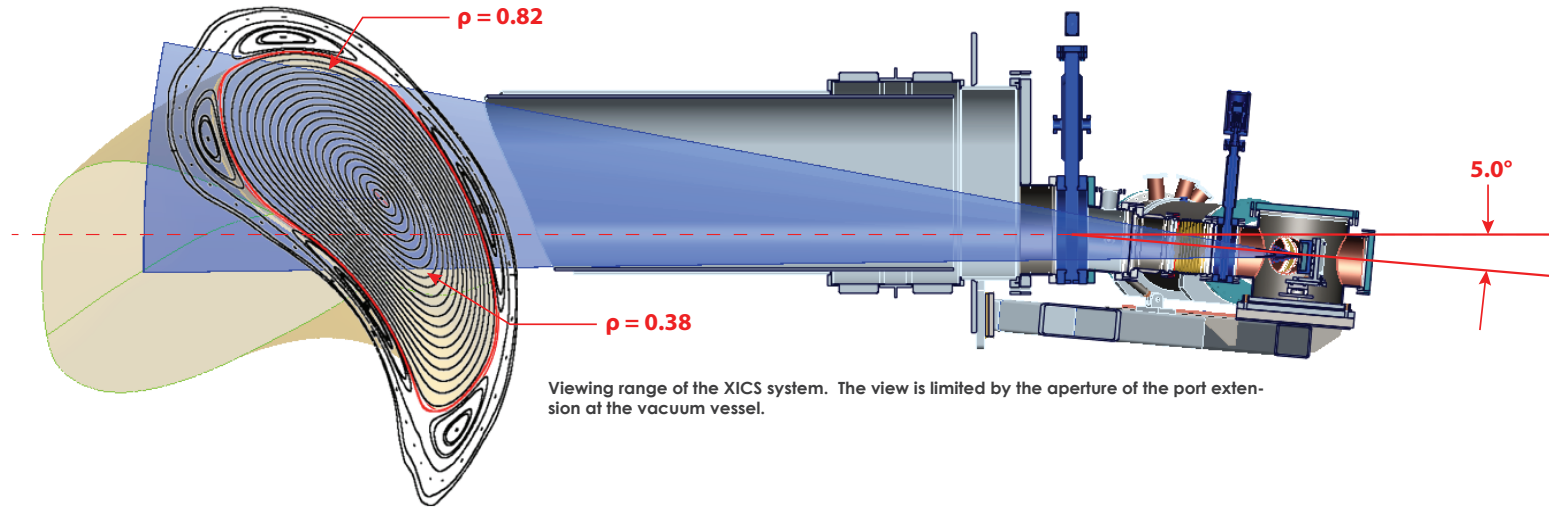
With low collisionalities and $T_e \gg T_i$ there are typically three possible E_r solutions:

- electron root ($E_r > 0$)
- ion root ($E_r < 0$)
- unstable root

Turbulent particle fluxes are expected to be intrinsically ambipolar.



PLASMA FLOW ON W7-X IS MEASURED USING AN X-RAY IMAGING CRYSTAL SPECTROMETER (XICS)



Viewing range of the XICS system. The view is limited by the aperture of the port extension at the vacuum vessel.

XICS can provide time resolved profile measurements of:

Ion temperature (T_i)

Electron temperature (T_e)

Perpendicular plasma flow (u_{\perp})

Argon impurity density (n_{Ar})

Relies on emission from highly charged ionization states of Argon (Ar^{16+}), which is seeded into the plasma for diagnostic purposes.

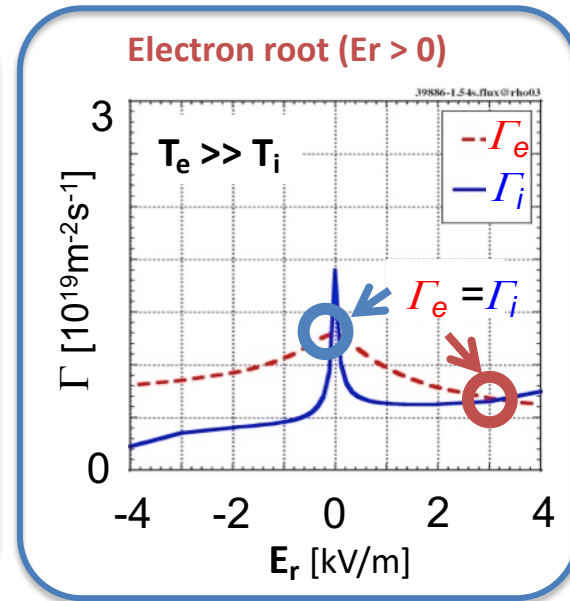
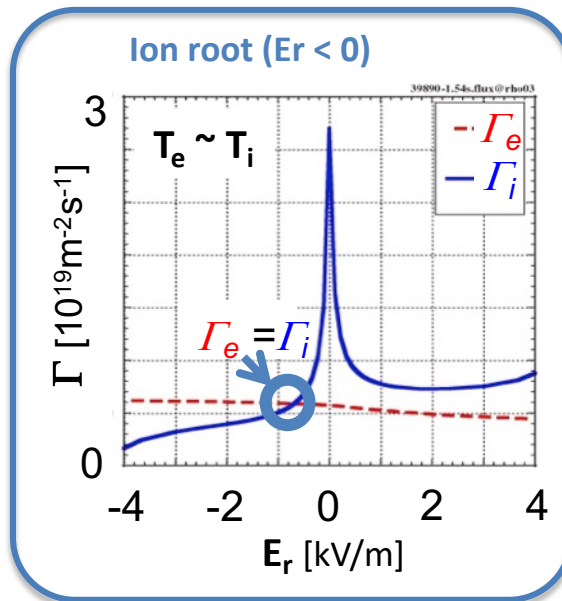
IN STELLARATORS THE RADIAL ELECTRIC FIELD PLAYS A SPECIAL ROLE IN PLASMA CONFINEMENT

Neoclassical ion and electron particle fluxes are affected by the radial electric field.

- Local ambipolarity is only consistent with particular values of E_r .

With low collisionalities and $T_e \gg T_i$ there are typically three possible E_r solutions:

- electron root ($E_r > 0$)
- ion root ($E_r < 0$)
- unstable root



PERPENDICULAR FLOW IS DIRECTLY RELATED TO THE RADIAL ELECTRIC FIELD THROUGH FORCE BALANCE

The radial force balance relates the perpendicular velocity and the radial electric field.

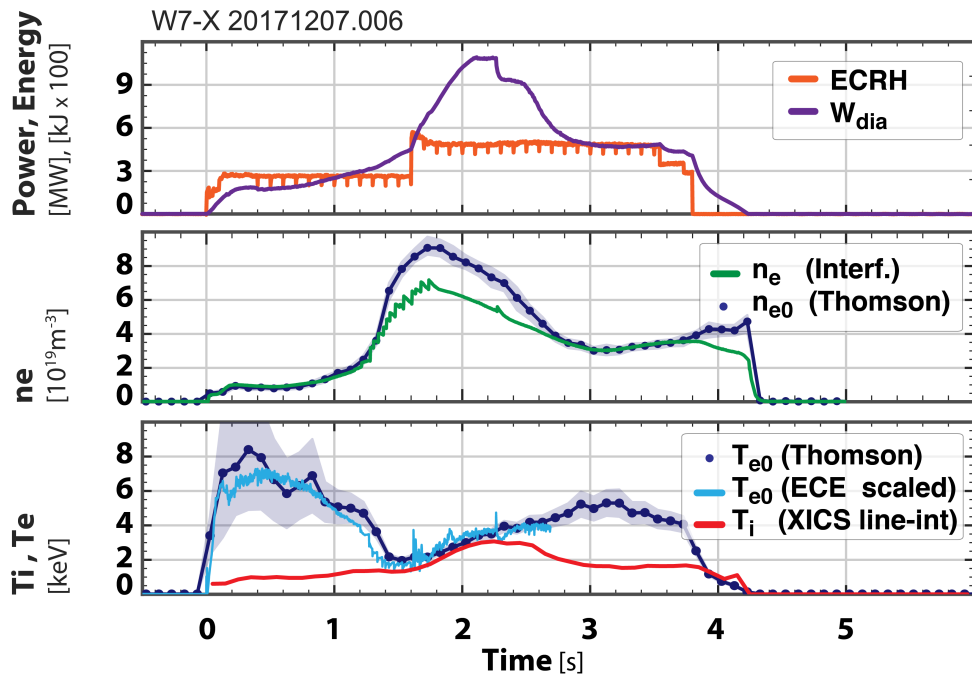
$$\langle E_r \rangle = \frac{1}{en_I Z_I} \frac{\partial p_I}{\partial \rho} \langle |\nabla \rho| \rangle - \langle u_{\perp} B \rangle$$

Pressure Gradient Term
(small)

Perpendicular Velocity
Term (from $u \times B$)

- Perpendicular velocity can be measured using the XICS diagnostic.
 - XICS is primarily sensitive to u_{\perp} due to the viewing geometry.
- The ion pressure gradient is small for flat ion pressures and weighted by the impurity charge.
 - Pressure gradient term is easily accounted for in both experimental and theoretical calculations.

PELLET FUELING ON W7-X HAS PRODUCED HIGH PERFORMANCE PLASMAS WITH $T_i \sim T_e$



- Only ECRH heating of electrons!

Injection of cryogenic hydrogen pellets has allowed access to high-performance plasmas characterized by:

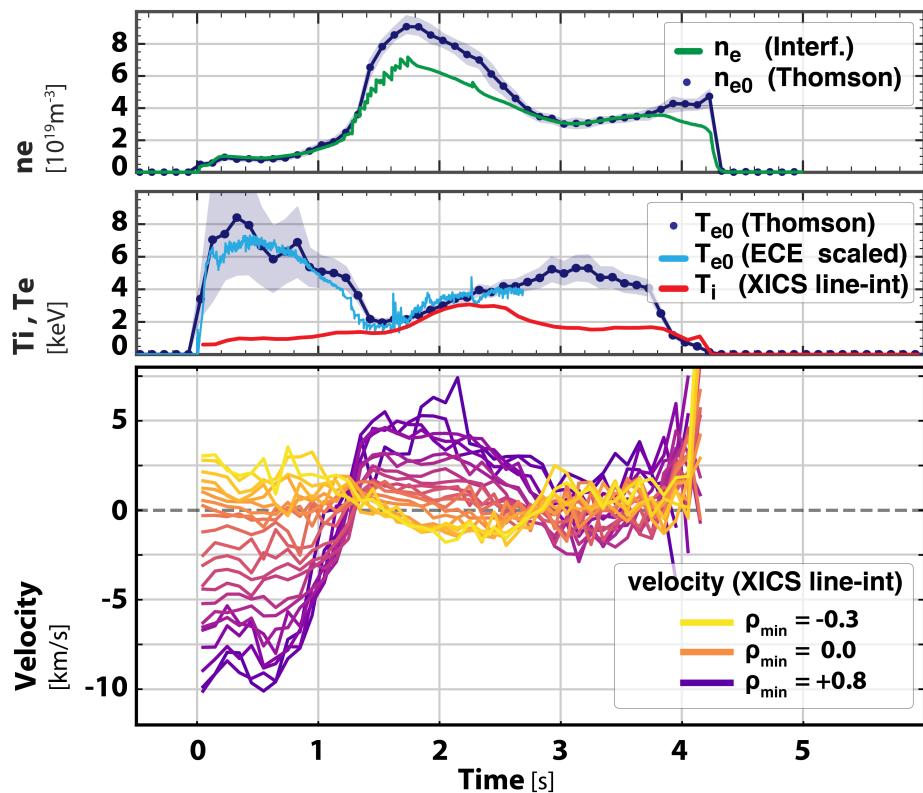
- Temperature equilibration ($T_e \sim T_i$)
- High densities density peaking
- Limited duration: 30 Hz for 1 second

Achieved parameters with pellet fueling:

- Density $n_{e0} \sim 1.0 \times 10^{20} \text{ m}^{-3}$
- Heating: 5MW ECRH
- Stored Energy: 1.1 MJ
- **Triple product: $0.6 \times 10^{20} \text{ m}^{-3} \text{ keV s}$**
(World record for stellarators)

This type of plasmas scenario can be reliably reproduced.

DRAMATIC CHANGES SEEN IN THE PERPENDICULAR PLASMA FLOW AS THE PLASMA PROFILES EVOLVE

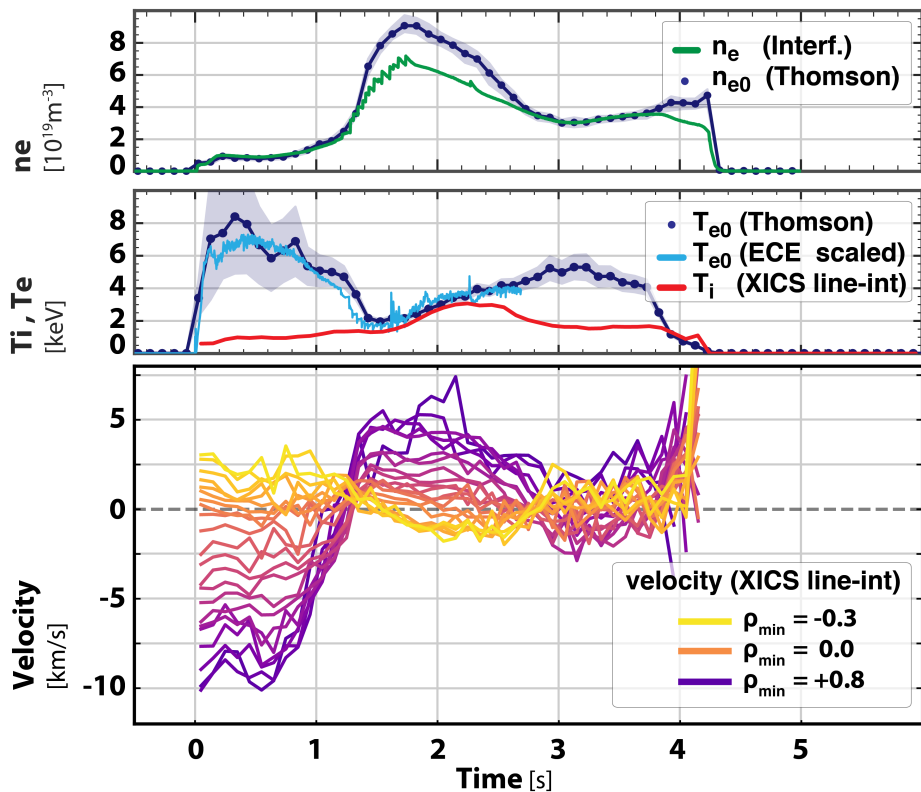


Changes in the perpendicular plasma rotation indicate that the radial electric field is evolving.

Evolution of the plasma rotation happens in sync with the evolution of the temperature and density profile.

- Expected behavior from neoclassical theory.

DRAMATIC CHANGES SEEN IN THE PERPENDICULAR PLASMA FLOW AS THE PLASMA PROFILES EVOLVE



Changes in the perpendicular plasma rotation indicate that the radial electric field is evolving.

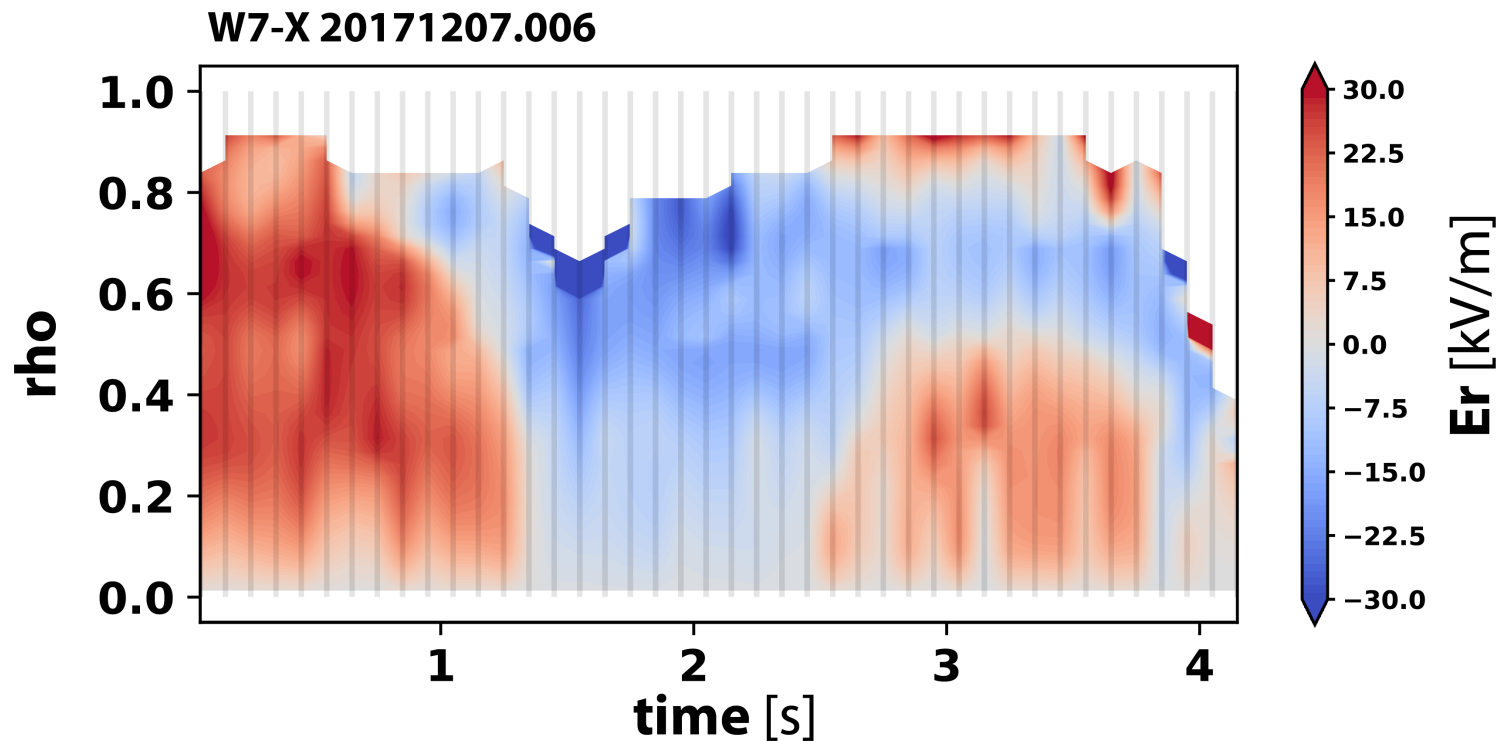
Evolution of the plasma rotation happens in sync with the evolution of the temperature and density profile.

- Expected behavior from neoclassical theory.

Tomographic inversion is used to find the perpendicular flow profile from the line-integrated measurements.

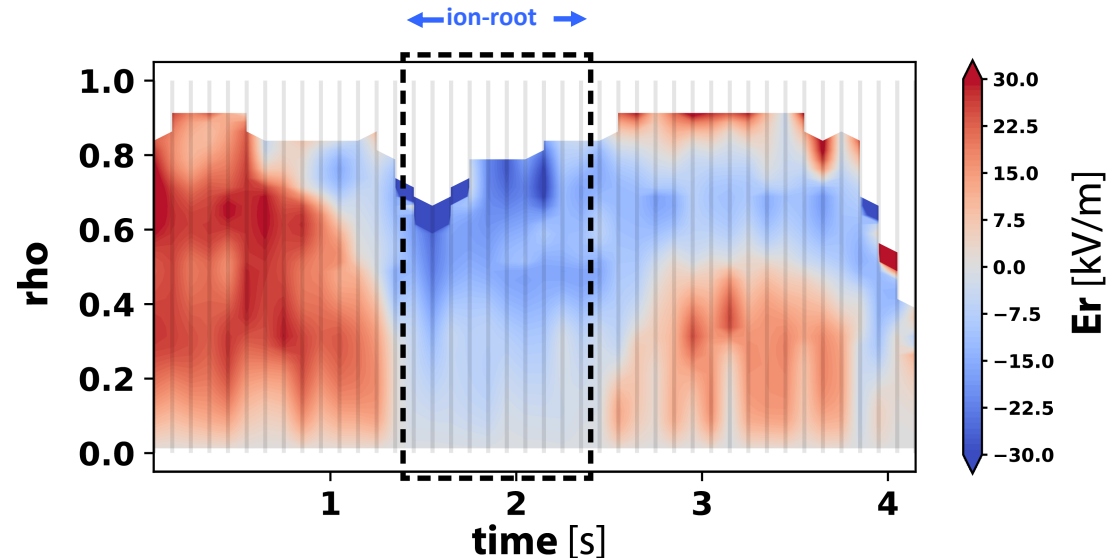
- Allows the E_r profile to be inferred

FIRST EXPERIMENTAL MEASUREMENTS OF ION-ROOT PLASMAS ON WENDELSTEIN 7-X

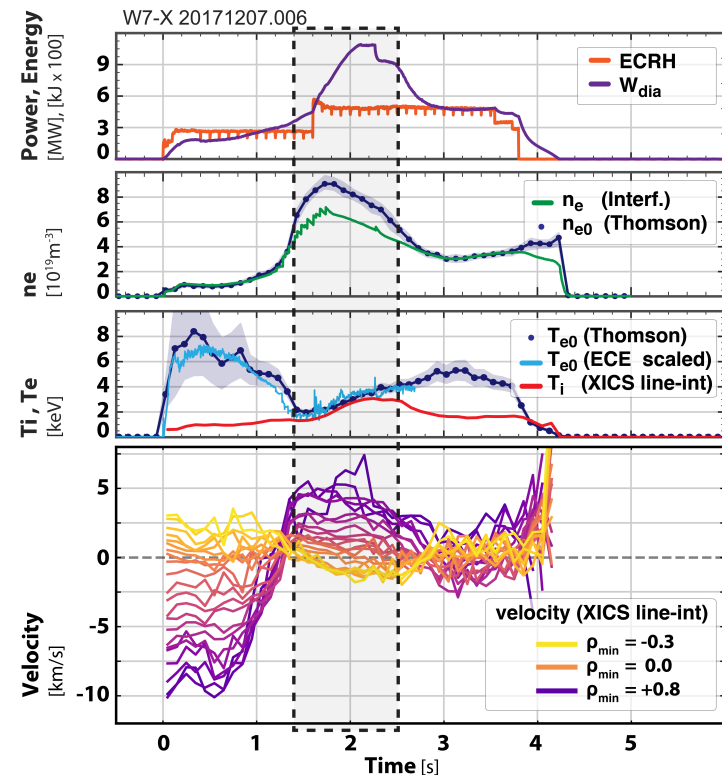


- Negative radial electric field \rightarrow **ion-root**

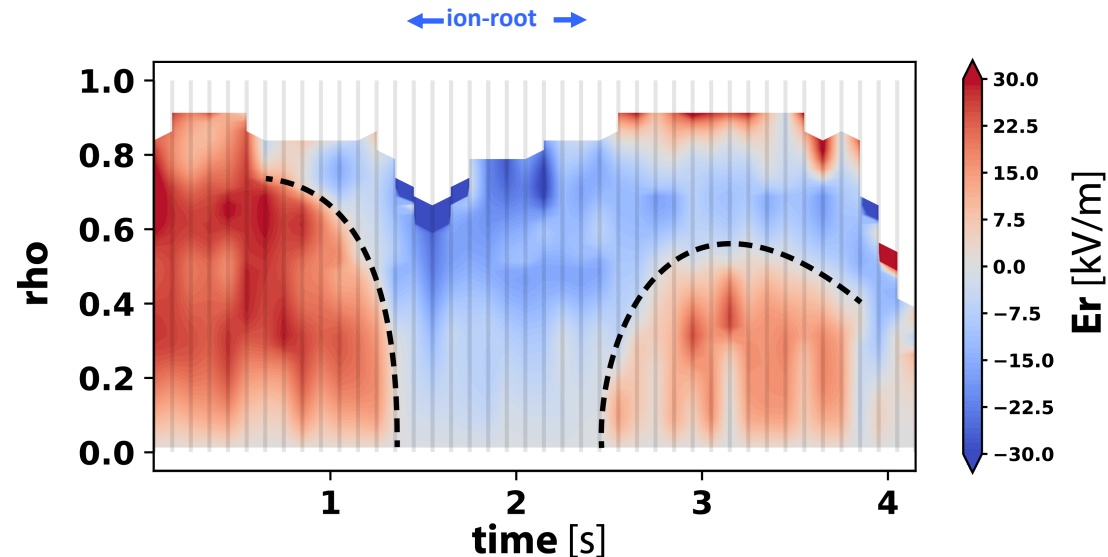
FIRST EXPERIMENTAL MEASUREMENTS OF ION-ROOT PLASMAS ON WENDELSTEIN 7-X



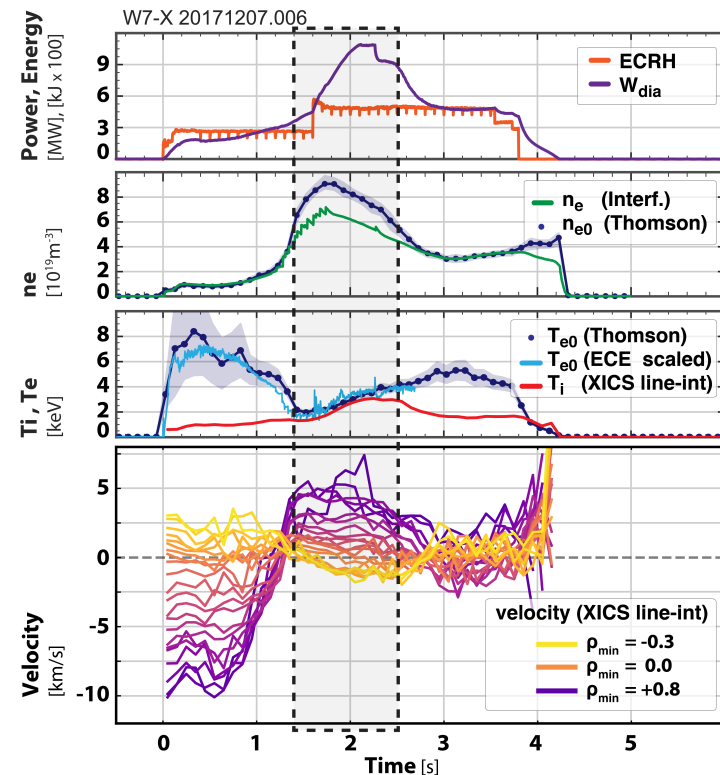
- Ion-root observed during the period when the ion and electron temperatures are equilibrated ($T_e \sim T_i$).



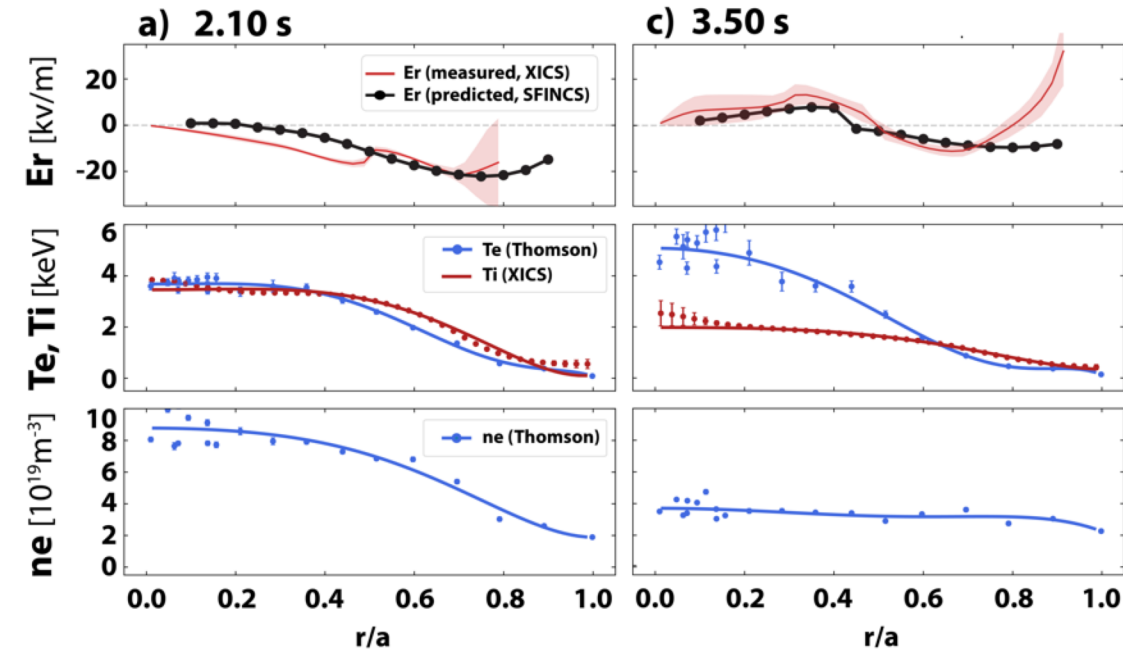
THE CROSSOVER RADIUS FROM ION-ROOT TO ELECTRON ROOT EVOLVES WITH THE PLASMA TEMPERATURES



- When $T_e \gg T_i$: E_r is in the electron-root over nearly the entire plasmas radius.
- As T_e approaches T_i : the electron-root region shrinks towards the plasma core.
- When $T_e \sim T_i$: E_r is in the ion-root.



NEOCLASSICAL PREDICTIONS OF THE RADIAL ELECTRIC FIELD MATCH THE MEASURED PROFILES



The ambipolar radial electric field can be predicted from the measured T_e , T_i and n_e profiles.

Neoclassical calculations by the SFINCS code:

- 4D Drift-Kinetic continuum code

Neoclassical predictions for E_r profiles show similar **structure and magnitude**.

- Good agreement over a wide range of plasma conditions.

Agreement between measurements and predictions of E_r profiles provides confidence in calculations of Neoclassical transport!

CONDITIONS FOR ACHIEVING ION ROOT

In program 20171207.006:

The ion-root phase is associated with:

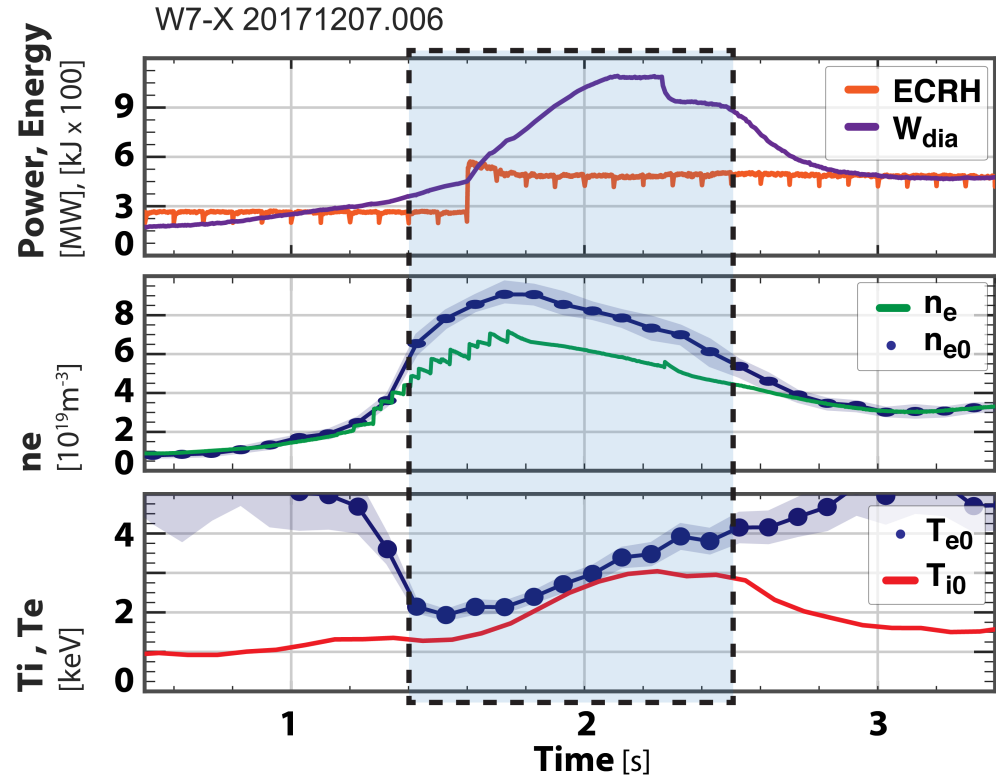
- Beginning of density peaking
- Temperature equilibration

At the start and end of the ion-root period the density is observed to be at the same value.

- n_e & $n_{e0} \sim 0.4 \times 10^{20} \text{ m}^{-3}$

ECRH power and plasma temperatures are dramatically different:

- Input power: 2MW vs. 5MW
- T_e & T_i : 1.5 keV vs. 3.0 keV



CONDITIONS FOR ACHIEVING ION ROOT

In program 20171207.006:

The ion-root phase is associated with:

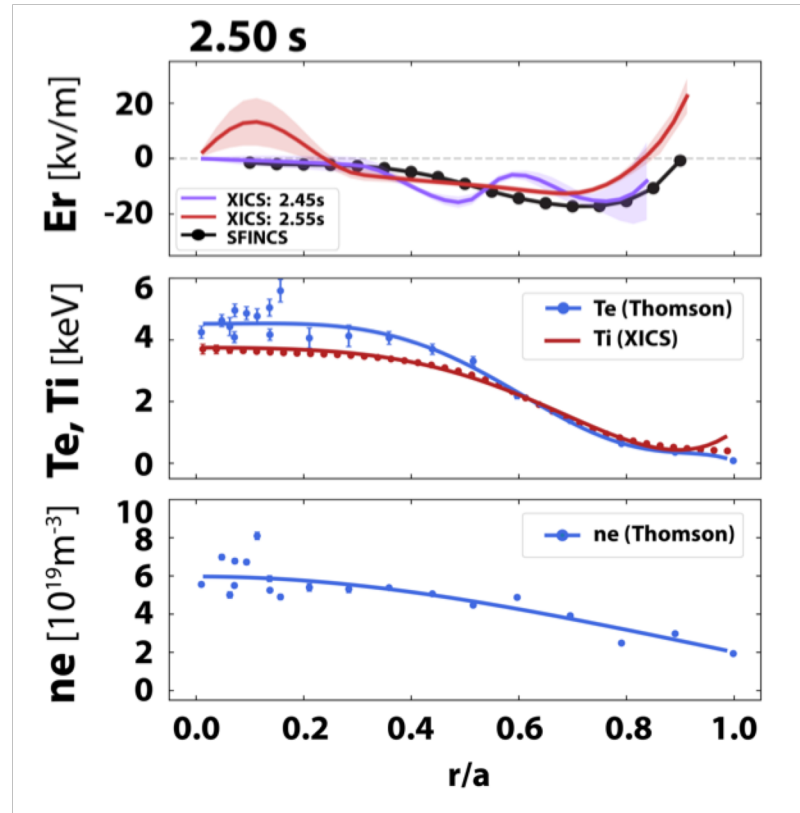
- Beginning of density peaking
- Temperature equilibration

At the start and end of the ion-root period the density is observed to be at the same value.

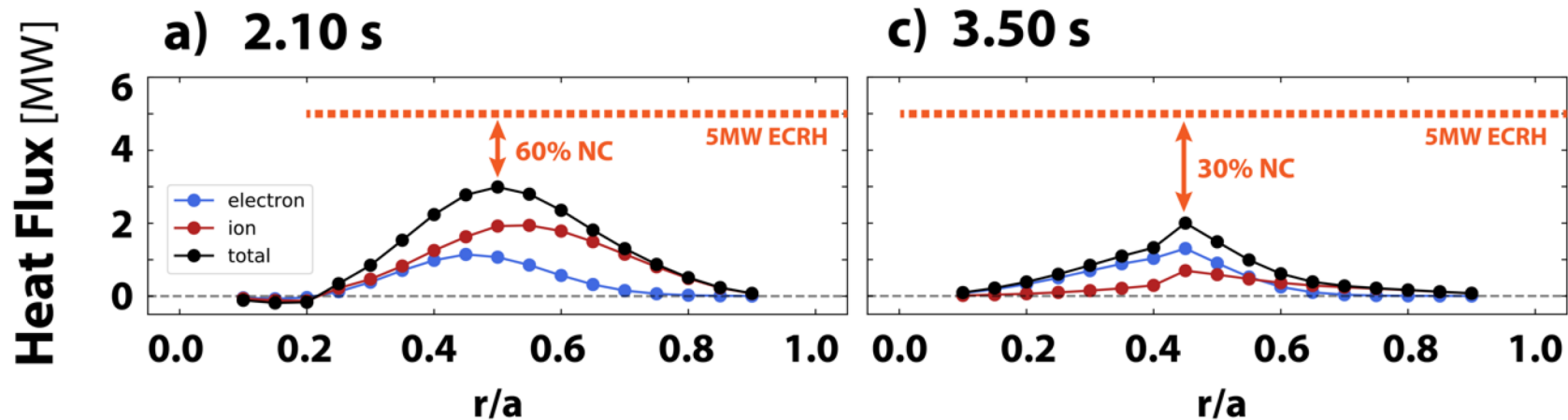
- n_e & $n_{e0} \sim 0.4 \times 10^{20} \text{ m}^{-3}$

ECRH power and plasma temperatures are dramatically different:

- Input power: 2MW vs. 5MW
- Te & Ti: 1.5 keV vs. 3.0 keV



A LARGER FRACTION OF THE TOTAL CORE TRANSPORT APPEARS TO BE NEOCLASSICAL DURING THE ION-ROOT PHASE



During **ion-root** phase (collisional coupled):

- Ion heat-flux is greater than electron heat-flux
- Neoclassical \approx 60% of total heat-flux

Neoclassical calculations have been made with several codes and show good agreement.

- SFINCS, DKES, NTSS, FORTEC-3D

During **electron-root** phase:

- Electron heat-flux is dominant.
- Neoclassical 20-30% of total heat-flux

IS A REDUCTION IN TURBULENT TRANSPORT RESPONSIBLE FOR THE IMPROVEMENT IN CONFINEMENT?

Electron density fluctuations are measured by the Phase Contrast Imaging (PCI) diagnostic.

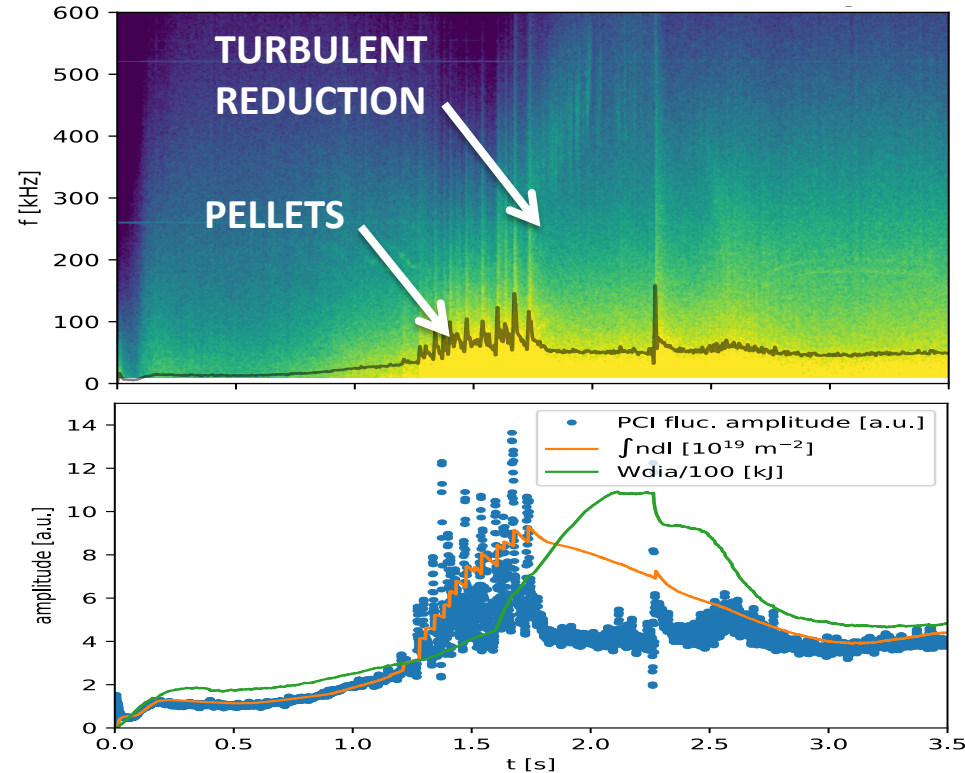
In W7-X, density fluctuations typically scale with the density ($\tilde{n}/n \sim \text{constant}$).

After pellet injection a clear reduction in the ratio of \tilde{n}/n is observed.

This reduction in turbulence may explain the improvement in core confinement.

Open question:

- Does the radial electric field play a direct role in changing the turbulent behavior?



IS A REDUCTION IN TURBULENT TRANSPORT RESPONSIBLE FOR THE IMPROVEMENT IN CONFINEMENT?

Electron density fluctuations are measured by the Phase Contrast Imaging (PCI) diagnostic.

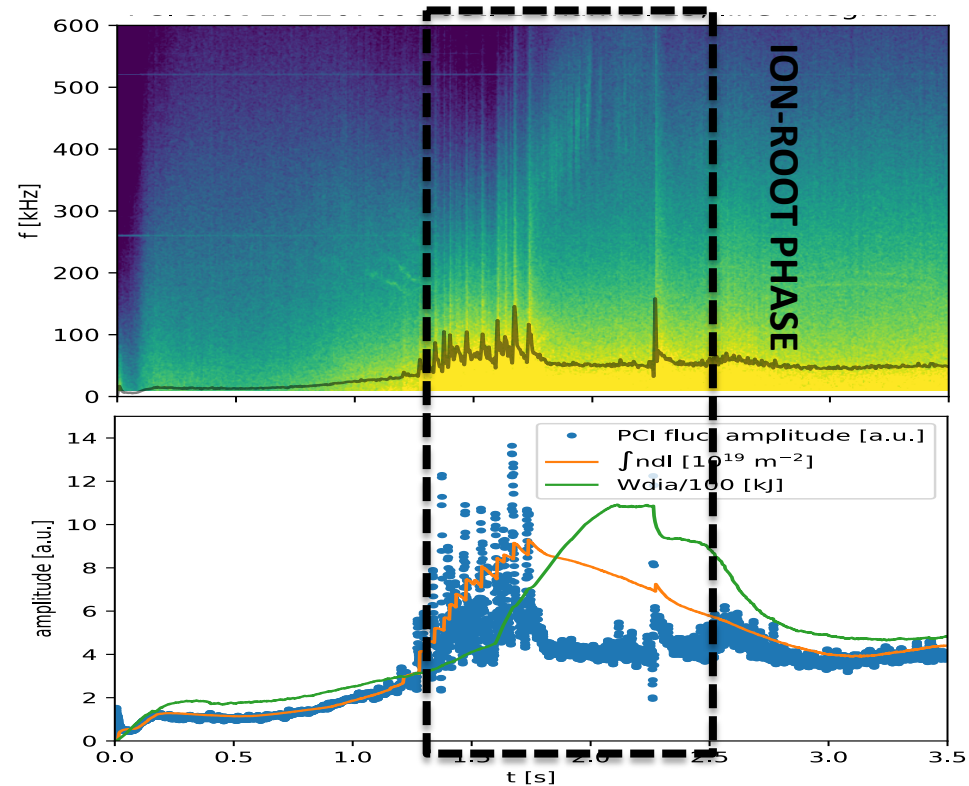
In W7-X, density fluctuations typically scale with the density ($\tilde{n}/n \sim \text{constant}$).

After pellet injection a clear reduction in the the ratio of \tilde{n}/n is observed.

This reduction in turbulence may explain the improvement in core confinement.

Open question:

- Does the radial electric field play a direct role in changing the turbulent behavior?



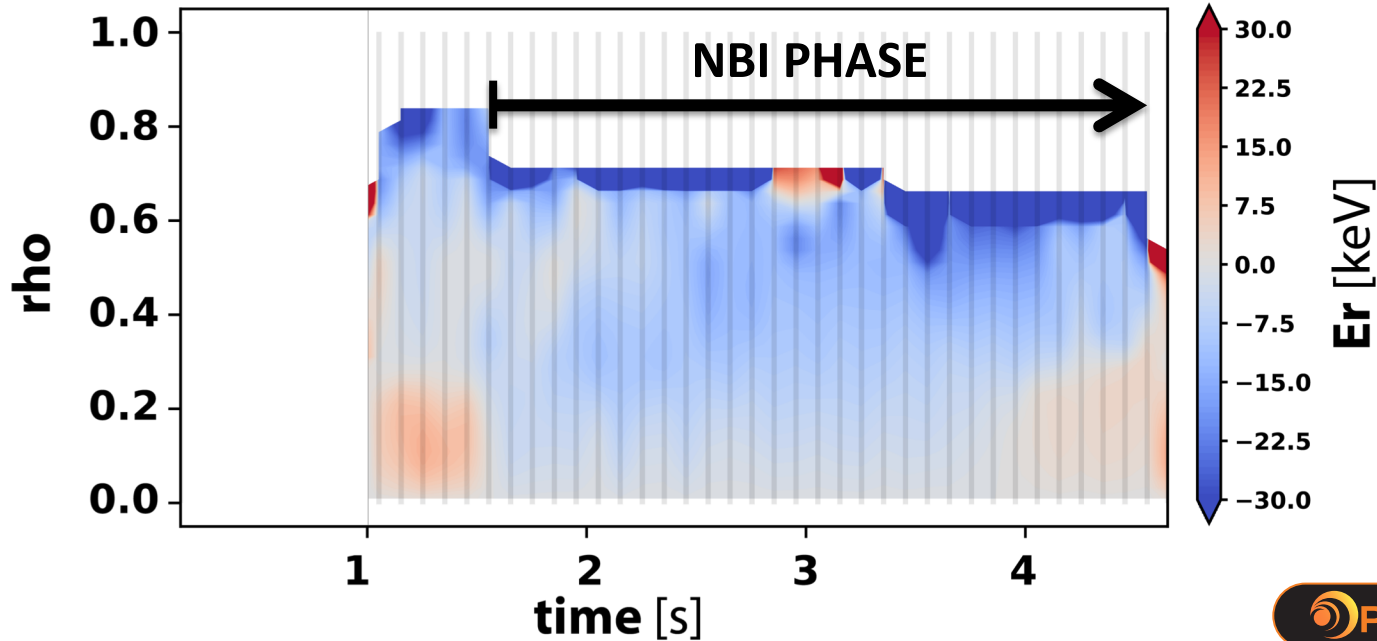
ACCESS TO ION-ROOT PLASMAS: NEUTRAL BEAM HEATING

Ion-root conditions can also be achieved with pure NBI heating.

- $T_i > T_e$, profiles have similar shape.
- 55 keV injection energy, 3.5 MW injected power.

NBI plasmas have several similarities to the pellet fueled discharges:

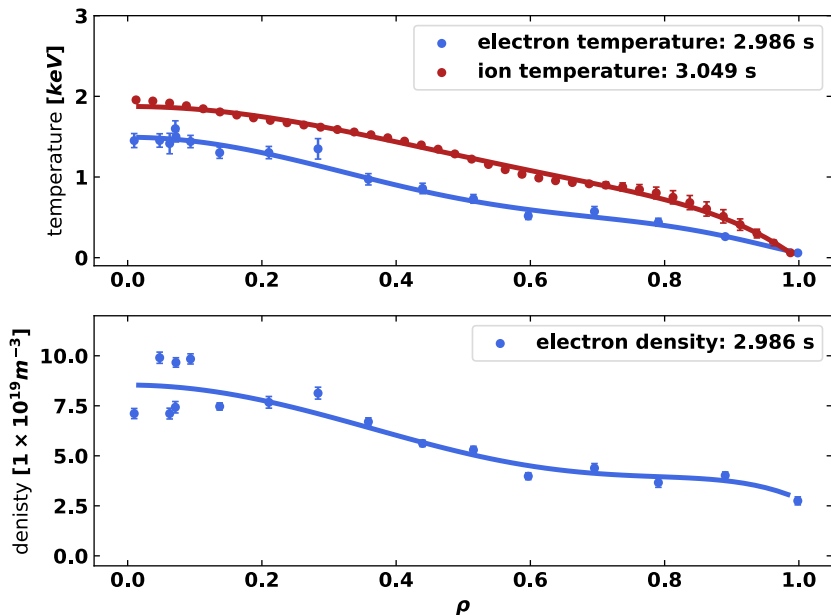
- High density with peaked density profiles
- Reduction in turbulent \tilde{n}/n observed



ACCESS TO ION-ROOT PLASMAS: NEUTRAL BEAM HEATING

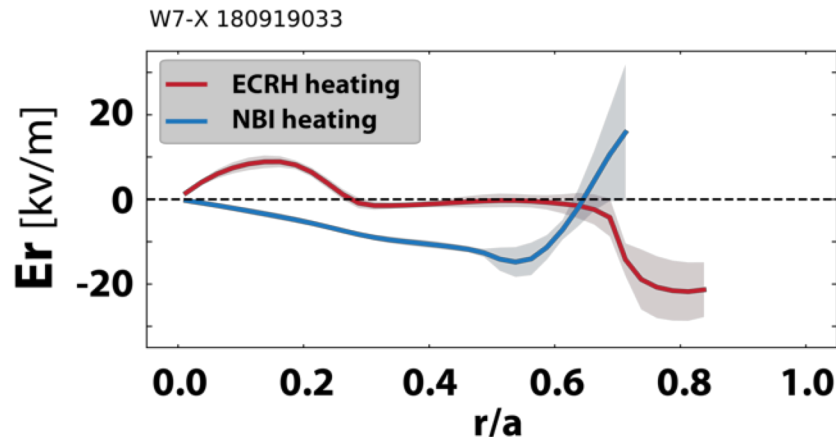
Ion-root conditions can also be achieved with pure NBI heating.

- $T_i > T_e$, profiles have similar shape.
- 55 keV injection energy, 3.5 MW injected power.



NBI plasmas have several similarities to the pellet fueled discharges:

- High density with peaked density profiles
- Reduction in turbulent \tilde{n}/n observed



ACCESS TO ION-ROOT PLASMAS: STEADY STATE WITH GAS FUELING? OFF-AXIS HEATING?

Steady state densities above $1.0 \times 10^{20} \text{ m}^{-3}$ can be achieved in W7-X through hydrogen gas fueling.

- Results in very flat density profiles.

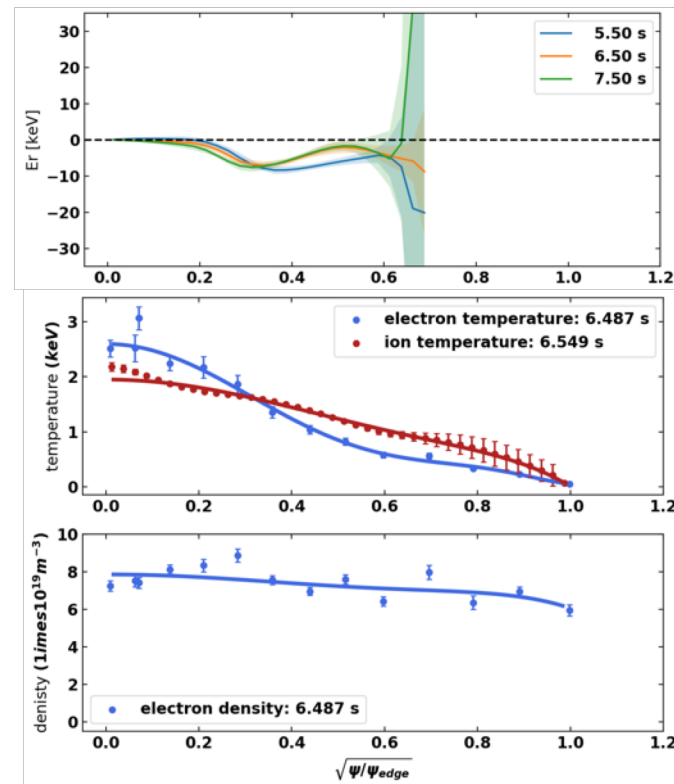
At these high densities it is possible to approach thermal equilibration.

- However, T_e and T_i profiles shapes are not generally similar.

Off-axis heating can also be used to bring the temperatures together by reducing and broadening the T_e profile.

Observations so far seem to indicate radial electric fields close to zero.

- Ion-root plasmas may have been achieved but further analysis is still required.



CONCLUSIONS

High-density **ion-root** plasmas have been observed in W7-X.

- These are the conditions for which W7-X has been optimized.
- (High beta operation not yet demonstrated.)

Equilibration between ions and electrons possible with only electron heating.

- $T_i \sim T_e$ achieved at high densities with both O2 and X2 ECRH heating.

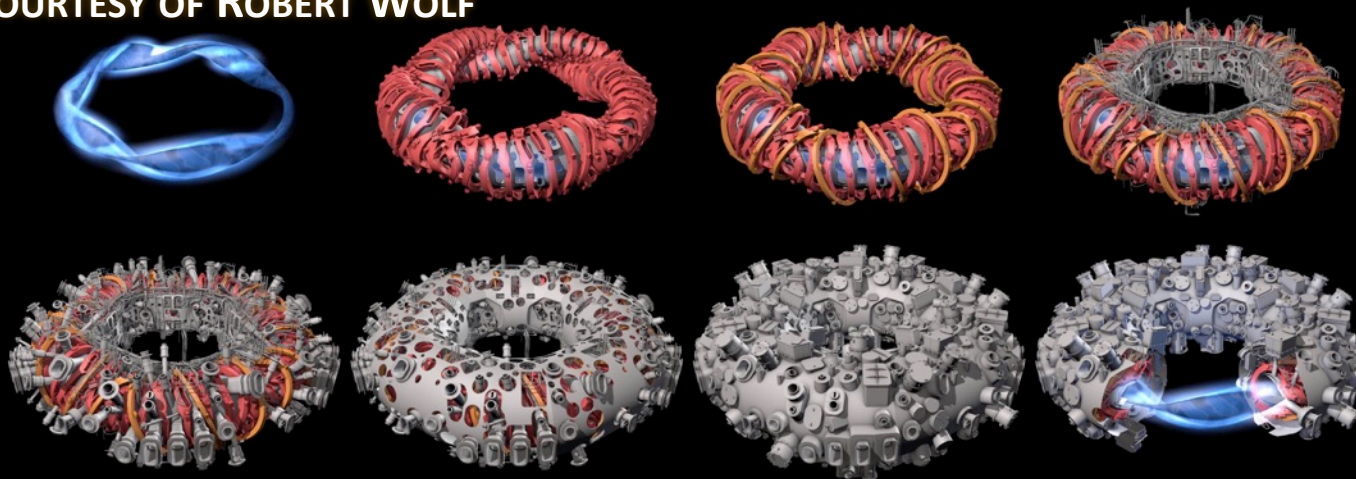
Good agreement between measured E_r profiles and neoclassical predictions.

- Agreement seen over a wide range of plasma conditions.
- Provides confidence in the validity of neoclassical calculations in W7-X.

PART 2: HIGHLIGHTS FROM THE FIRST W7-X DIVERTOR CAMPAIGN

NOVIMIR PABLANT ON BEHALF OF THE W7-X TEAM

SLIDES COURTESY OF ROBERT WOLF



WENDELSTEIN 7-X HAS BEEN OPTIMIZED WITH RESPECT TO A NUMBER OF DIFFERENT PARAMETERS

The plasma shape and coil set have been optimized:

1. High quality vacuum magnetic surfaces
2. Good finite equilibrium properties
3. **Reduced Neoclassical transport**
4. Plasma stability up to $\langle \beta \rangle \sim 5\%$
5. Minimization of bootstrap current and Shafranov shift
6. Good collisionless fast particle confinement
7. Modular coil feasibility

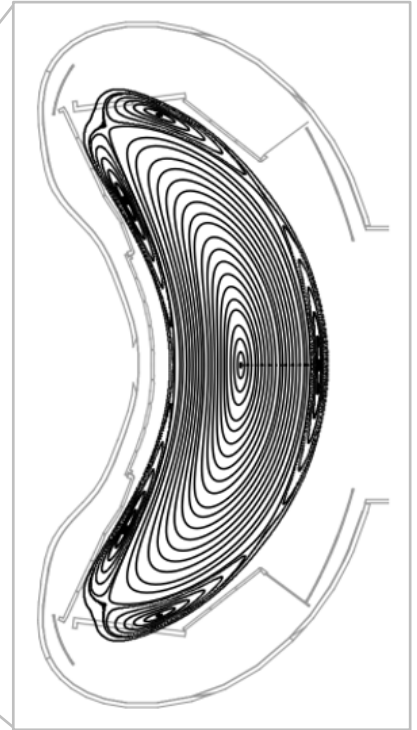
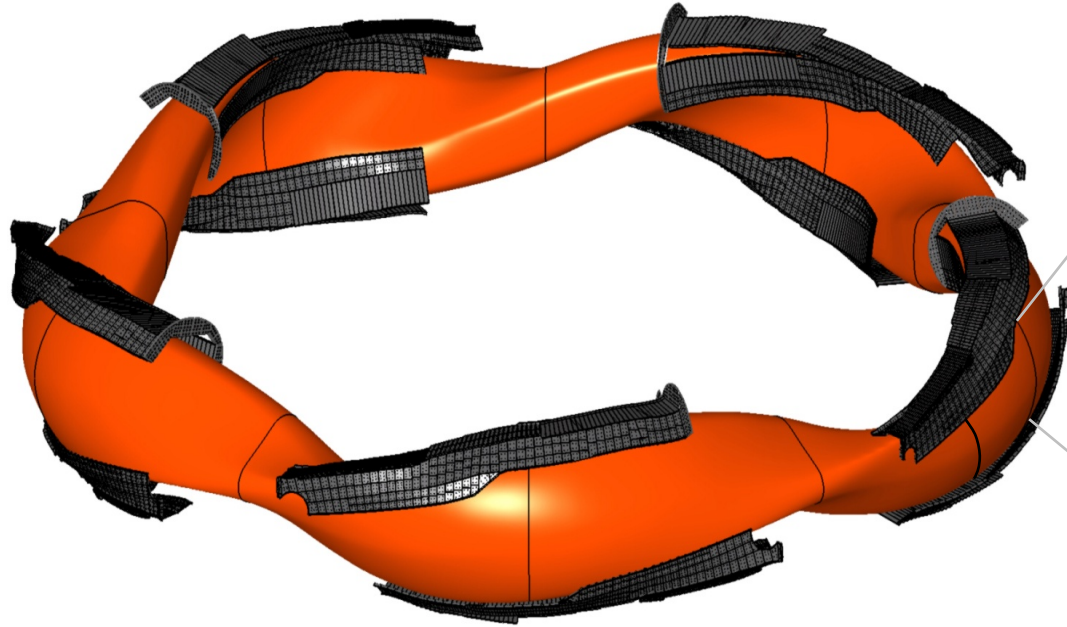
Physics research goals:

- **Verify stellarator optimizations**
- Verify performance of island divertor design
- Demonstrate plasma density control at high densities
- Explore impurity confinement

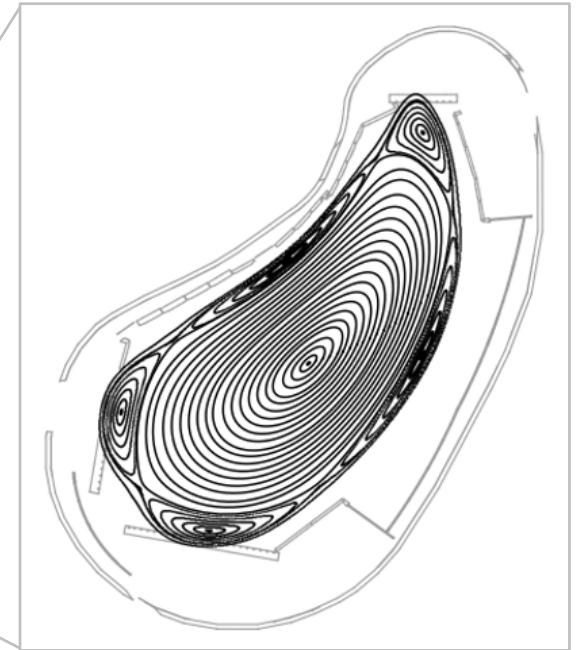
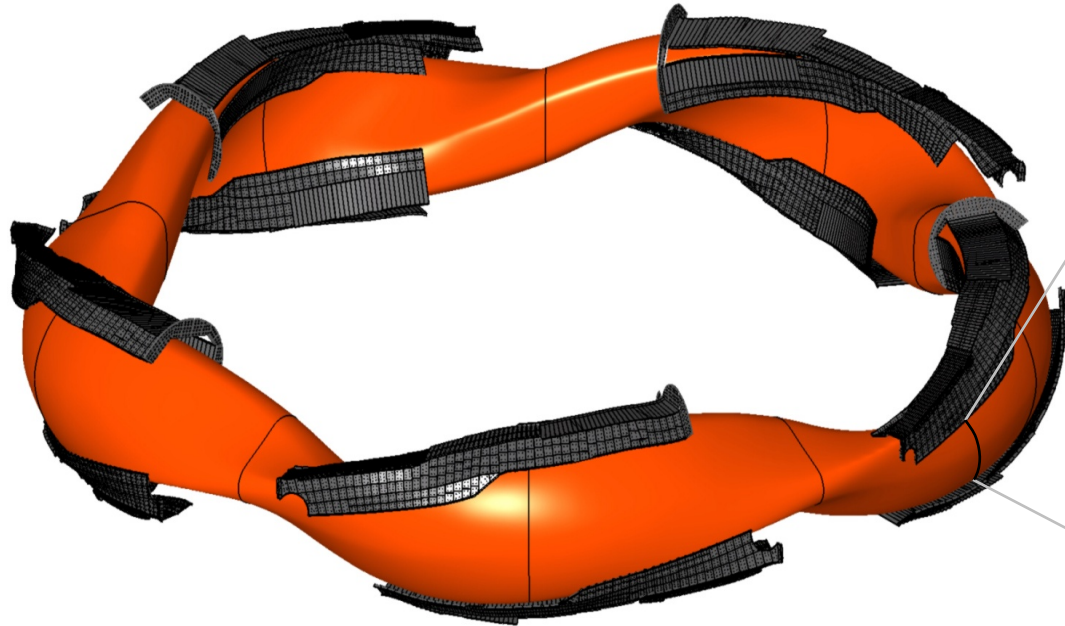
Engineering research goals:

- **Sustain high density, high performance steady state operation.**
- Demonstrate steady state high heat flux handling

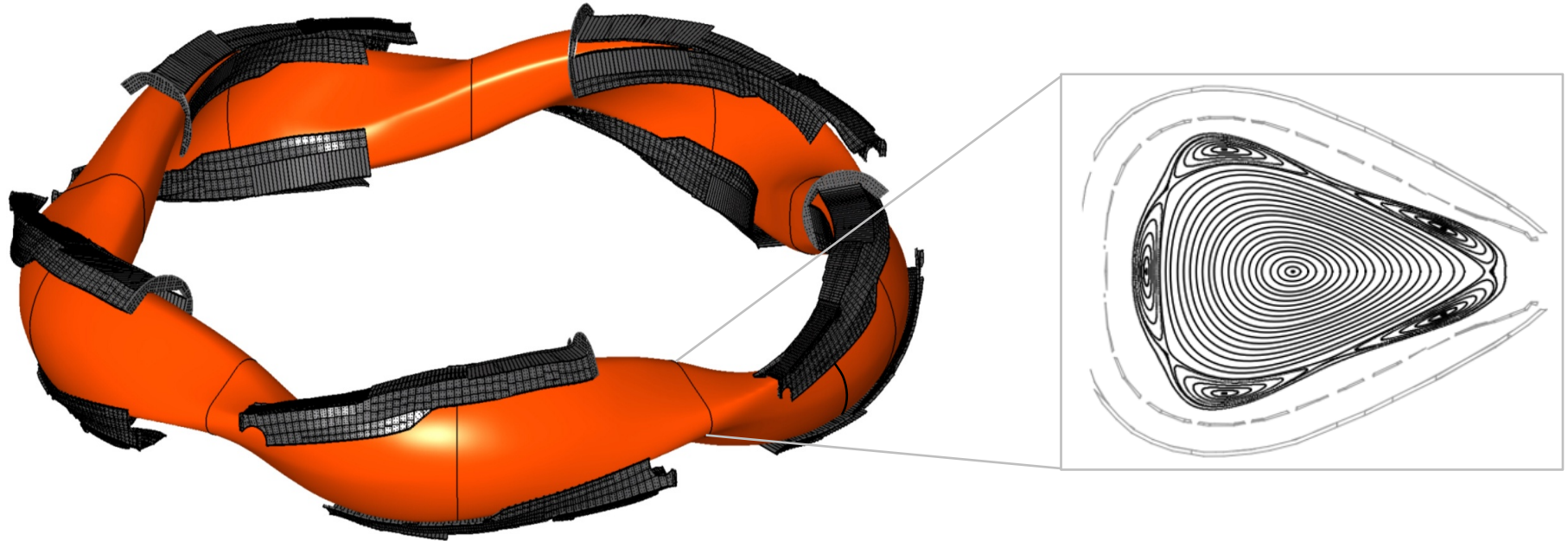
Controlled heat and particle exhaust using open magnetic field lines intersecting dedicated target plates



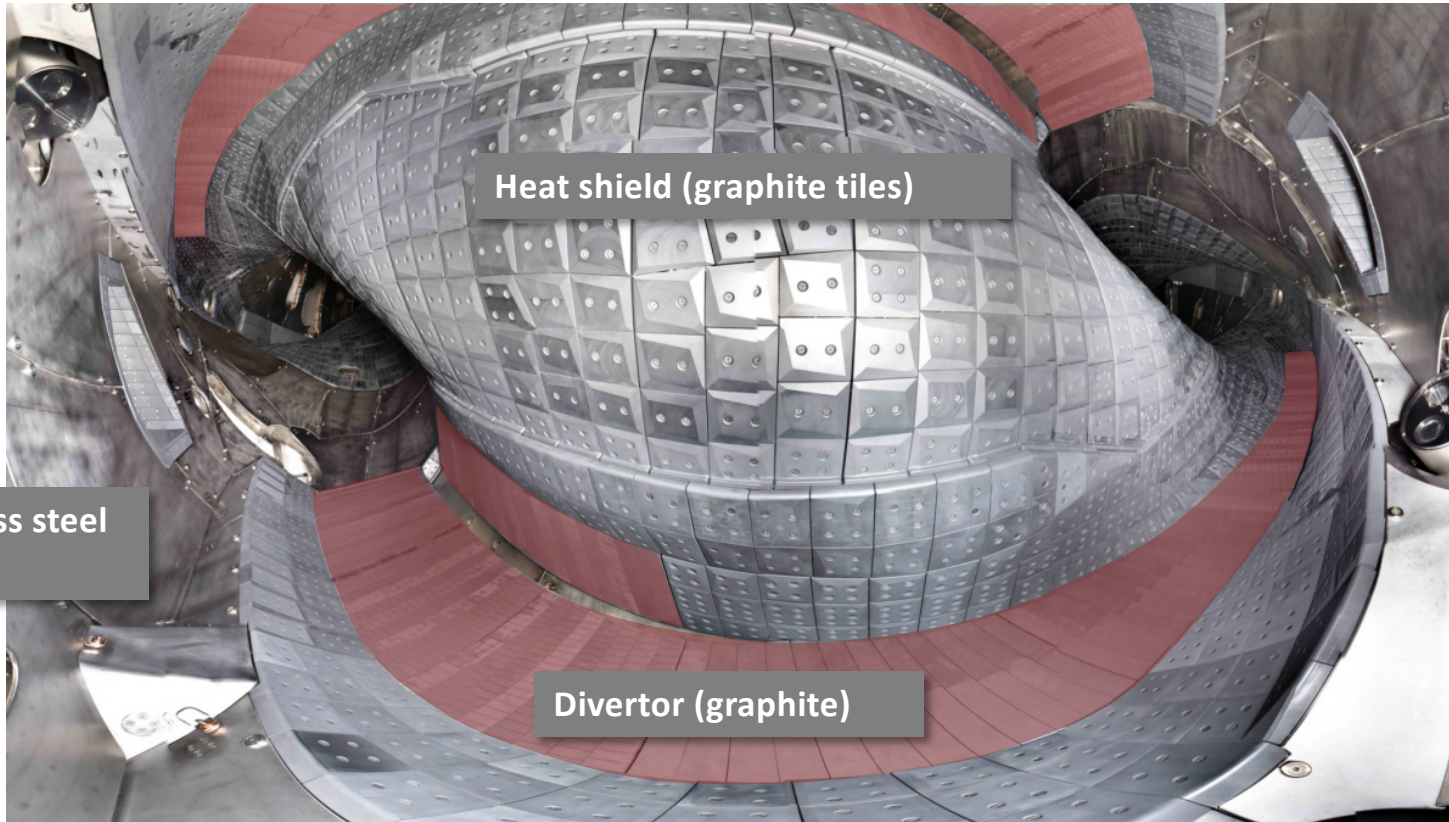
Controlled heat and particle exhaust using open magnetic field lines intersecting dedicated target plates



Controlled heat and particle exhaust using open magnetic field lines intersecting dedicated target plates



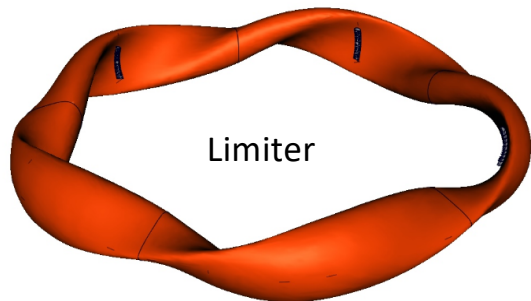
Fisheye view into the plasma vessel



Heat shield (graphite tiles)

Stainless steel
panels

Divertor (graphite)



Limiter

OP 1.2: 2017 / 2018

Uncooled divertor configuration

$$P_{\text{ECRH}} < 8 \text{ MW}$$

$$P_{\text{NBI}} < 4 \text{ MW}$$

$$\int P \, dt \leq 80 \text{ MJ} \dots 200 \text{ MJ}$$

$$\tau_{\text{pulse}} \sim 10 \text{ s} \dots 100 \text{ s}$$

OP 1.1: 2015 / 2016

Limiter configuration

$$P_{\text{ECRH}} < 5 \text{ MW}$$

$$\int P \, dt \leq 4 \text{ MJ}$$

$$\tau_{\text{pulse}} \sim 1 \text{ s}$$

OP 2: 2021 ...

Steady-state operation

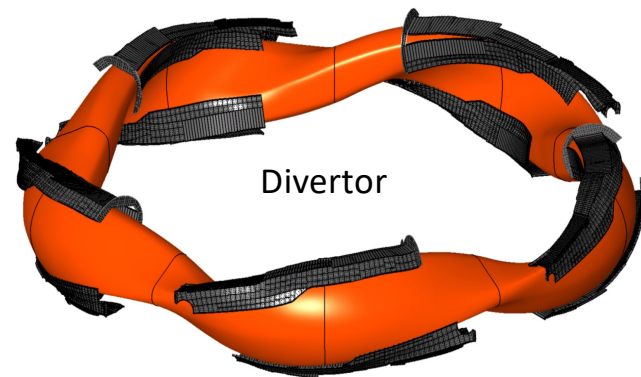
Actively cooled divertor configuration

$$P_{\text{ECRH}} \sim 10 \text{ MW (cw)}$$

$$P_{\text{NBI}} \sim 10 \text{ MW}, P_{\text{ICRH}} \sim 2 \text{ MW (10 s)}$$

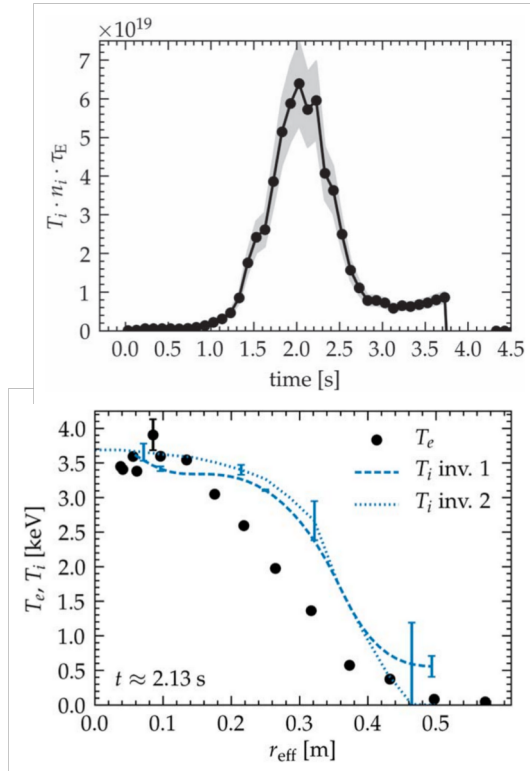
$$P/A \leq 10 \text{ MW/m}^2$$

Technical limit **30 minutes** @ 10 MW



Divertor

Record triple product achieved with X2-ECRH and pellets



Density increase by pellets and ECRH below X2 cut-off density

- 5 MW ECRH (max. 7 MW)
- $n_e \leq 1 \times 10^{20} \text{ m}^{-3}$
- $T_i = T_e \leq 3.8 \text{ keV}$
- Central β reaches 3.7 %
- Energy confinement time $\tau_E \leq 220 \text{ ms}$ ($1.4 \times \tau_{ISS04}$)

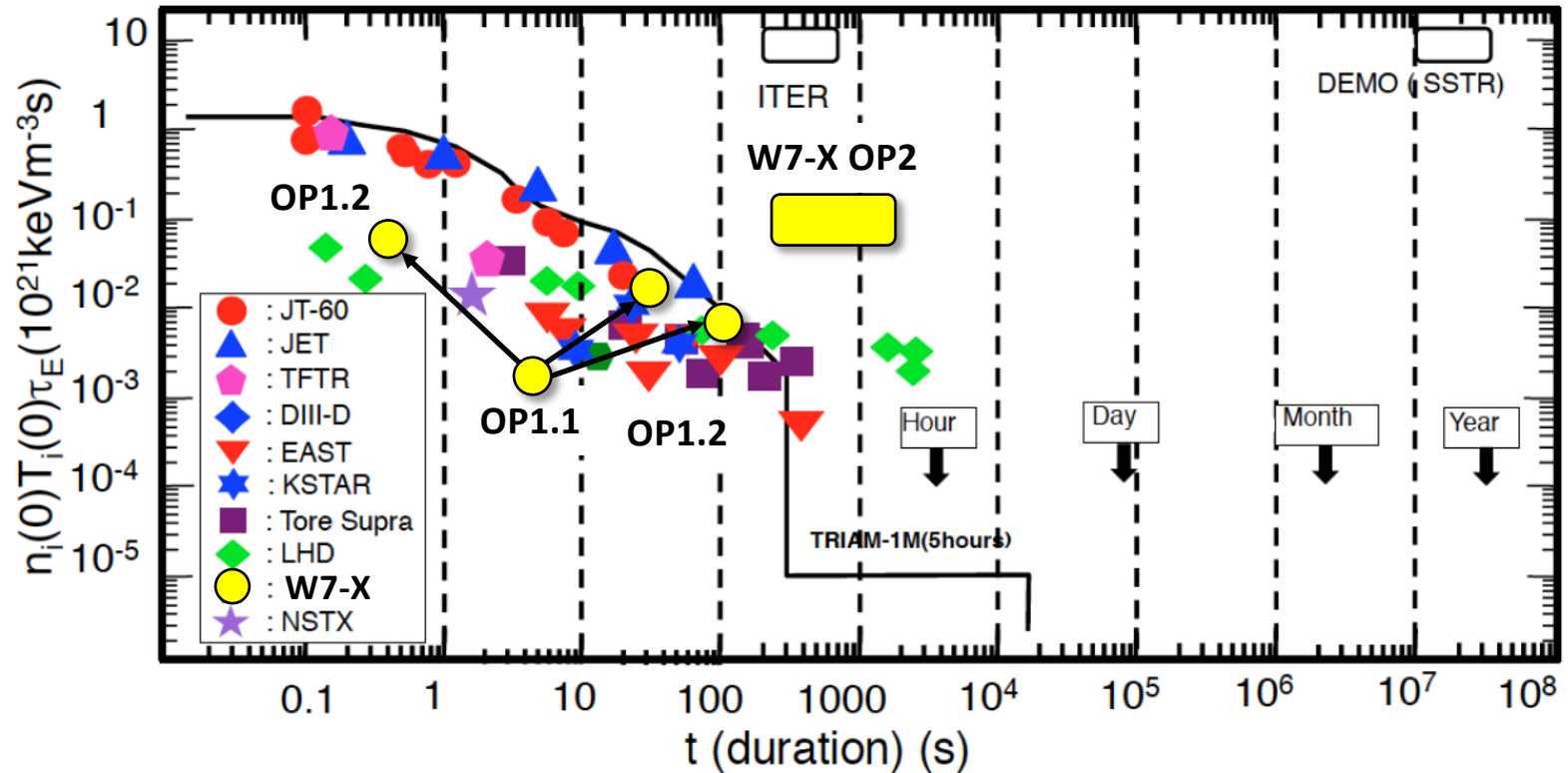
Record triple product for stellarators (transiently)

$$n T_i T_e \sim 6.8 \times 10^{19} \text{ keV m}^{-3} \text{ s}$$

Highest triple product to date (in large tokamaks, transiently)

$$n T_i T_e \sim 10^{21} \text{ keV m}^{-3} \text{ s}$$

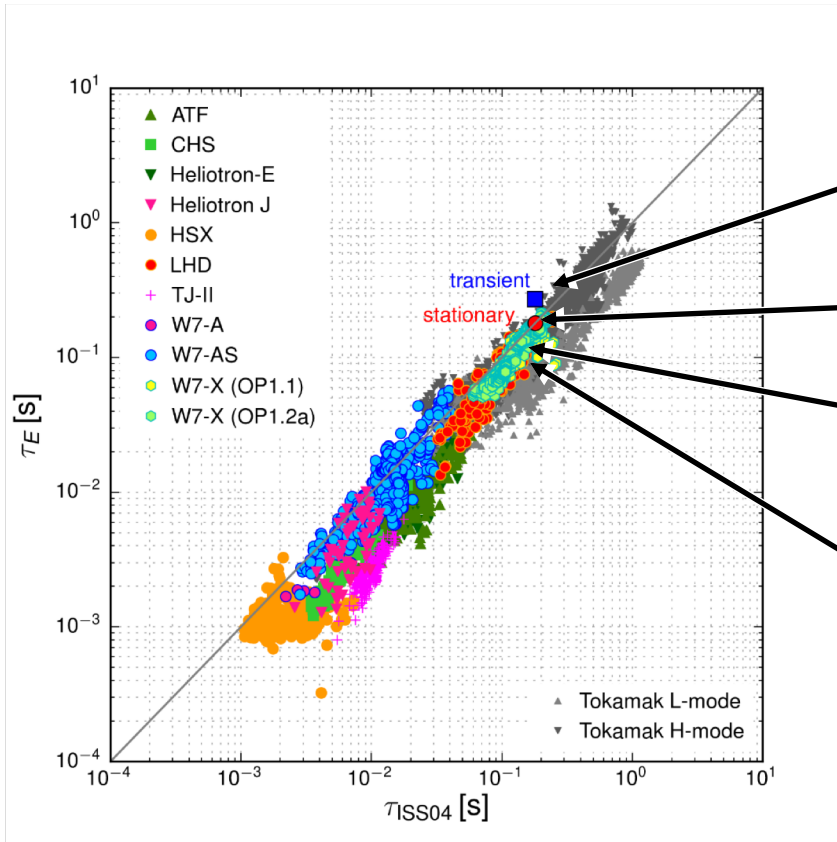
On the way to high performance steady-state operation



Courtesy of M. Kikuchi

T. Sunn Pedersen et al, Phys. Plasmas 24 (2017) 055503

Scaling of energy confinement time



Record divertor (OP1.2) plasma (transient)

Stationary divertor (OP1.2) plasma

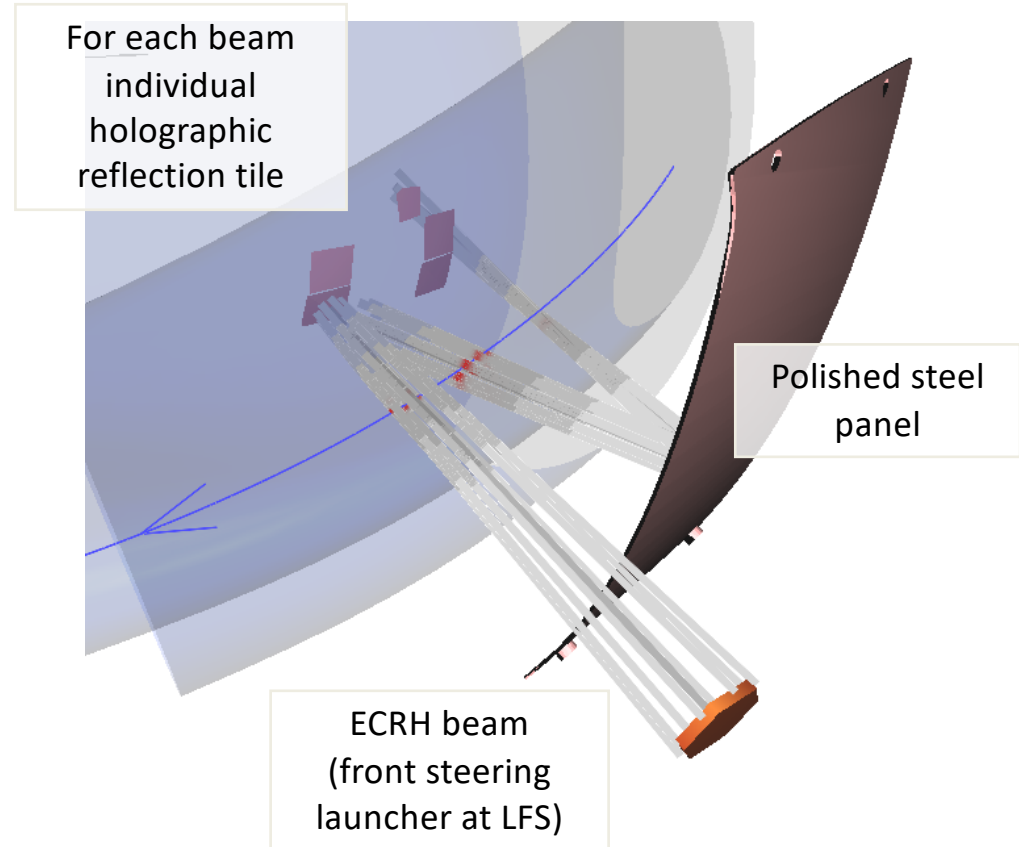
Divertor plasma (OP1.2) data

Limiter plasma (OP1.1) data

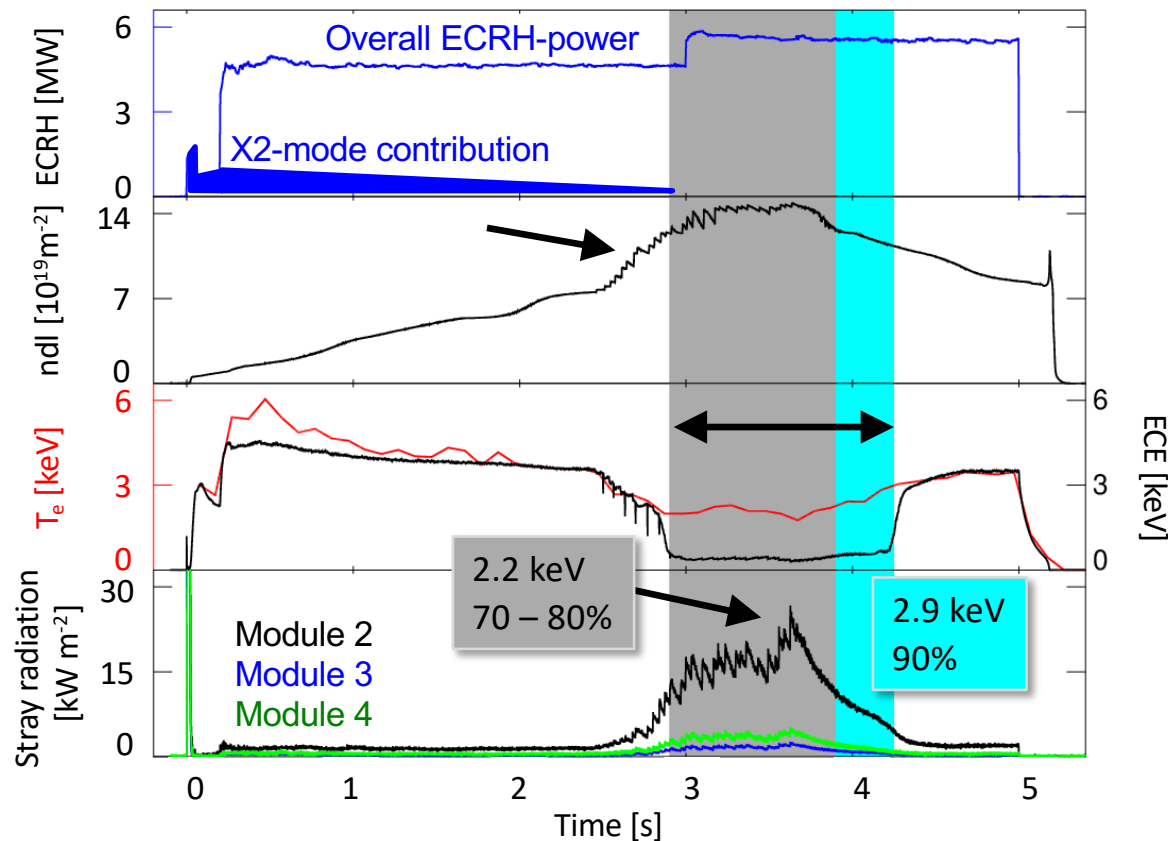
$$\tau_E^{\text{ISS04}} = 0.134 a^{2.28} R^{0.64} P^{-0.61} \bar{n}_e^{-0.54} B^{0.84} t_{2/3}^{0.41}$$

O2-ECRH requires a multi-pass absorption scheme

- X2-mode ECRH up to cut-off $< 1.2 \cdot 10^{20} \text{ m}^{-3}$
- For higher densities O2-mode polarization
- O-mode requires multi-pass absorption (single beam absorption $\sim 70\%$)
- Special holographic mirrors guarantee defined beam path through plasma centre (covered by tungsten)



First demonstration of O2-ECRH above X2 cut-off



Startup in X2-mode
Add O2-mode
Change X2 to O2

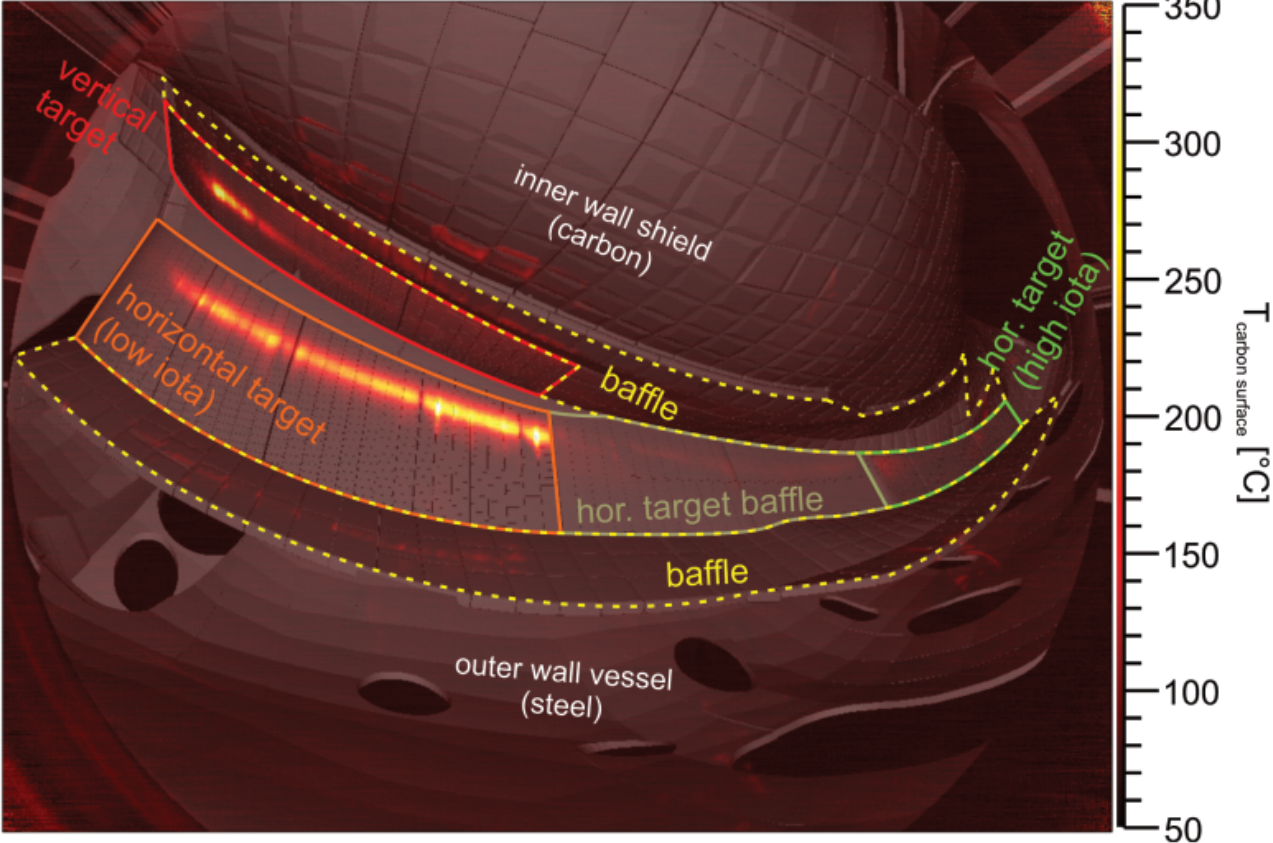
Increase of density
with pellets

ECE close to 140 GHz
indicates cut-off:
 $n_{e0} \approx 1.5 \times 10^{20} \text{ m}^{-3}$

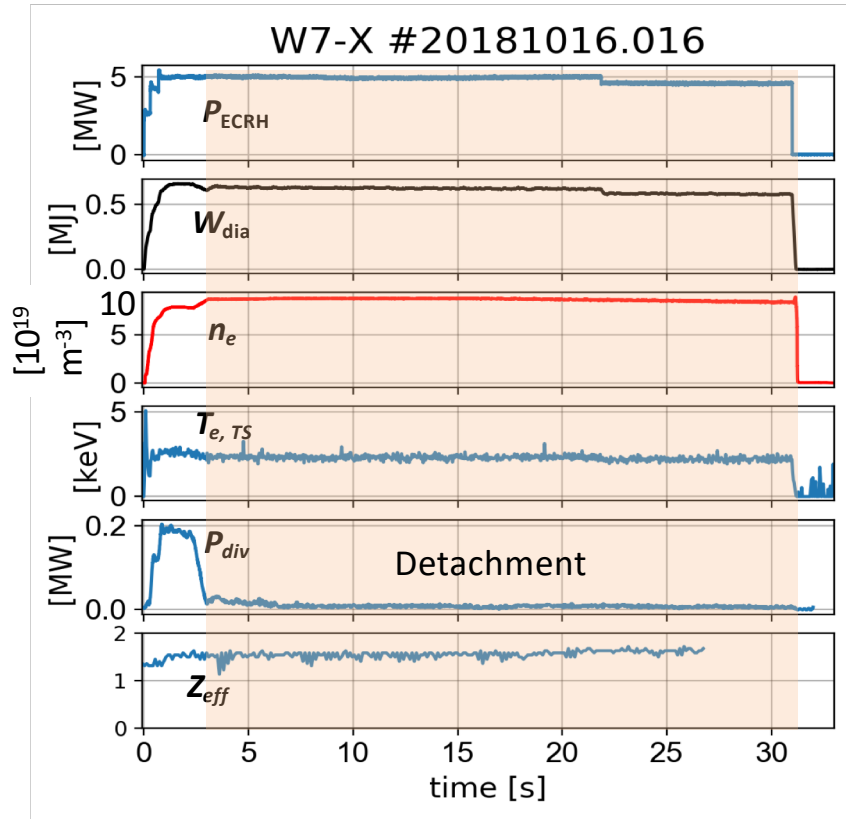
Stray radiation still
acceptable $< 50 \text{ kW/m}^2$
Absorption $\sim T_e^2$

T. Stange, PO5.00002

Infra-red observation of all 10 divertor modules

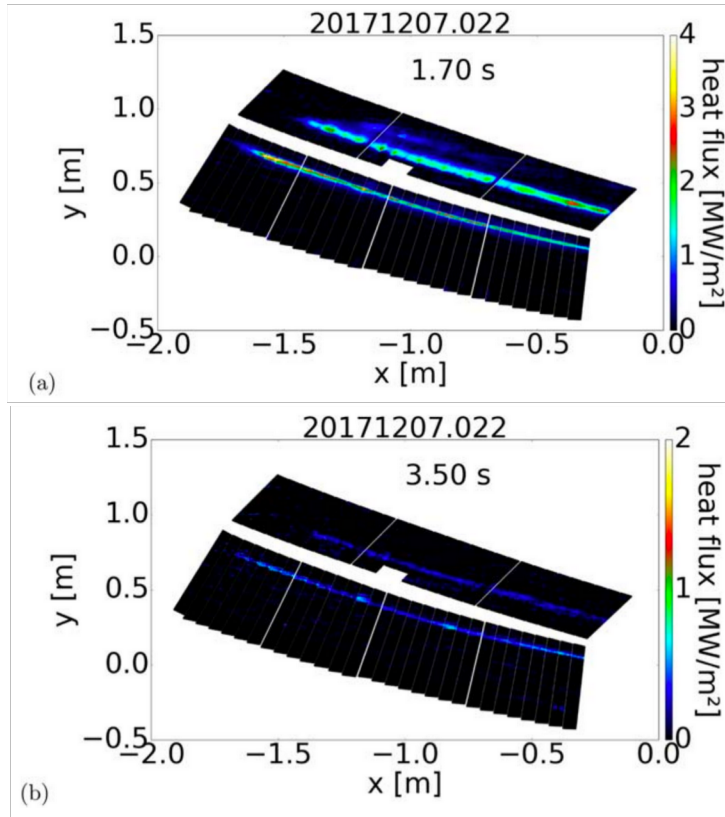


Detachment across all 10 divertor modules over half a minute



- 5 MW of O2-ECRH heating (150 MJ)
- Interferometer based density feedback control
- Pulse duration not limited by plasma performance
- Divertor neutral pressure $\sim 6\text{-}7 \times 10^{-4}$ mbar
- Z_{eff} stays roughly constant.

Detachment across all 10 divertor modules over half a minute

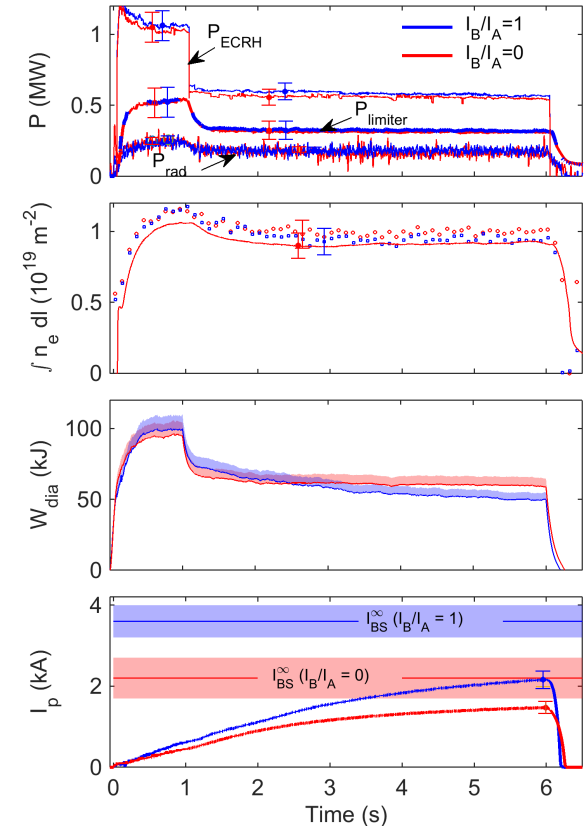


- 5 MW of O2-ECRH heating (150 MJ)
- Interferometer based density feedback control
- Pulse duration not limited by plasma performance
- Divertor neutral pressure $\sim 6\text{-}7 \times 10^{-4}$ mbar
- Z_{eff} stays roughly constant.

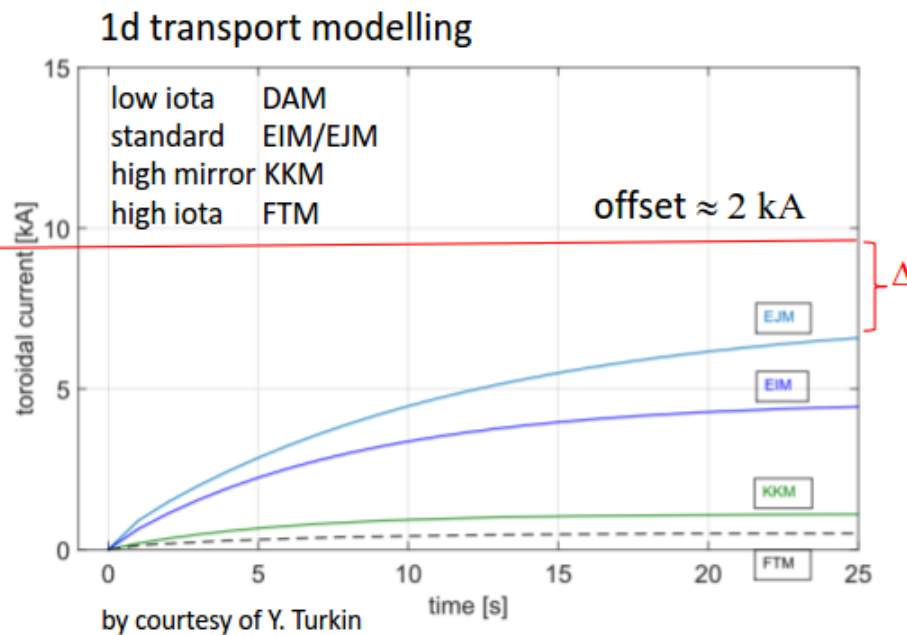
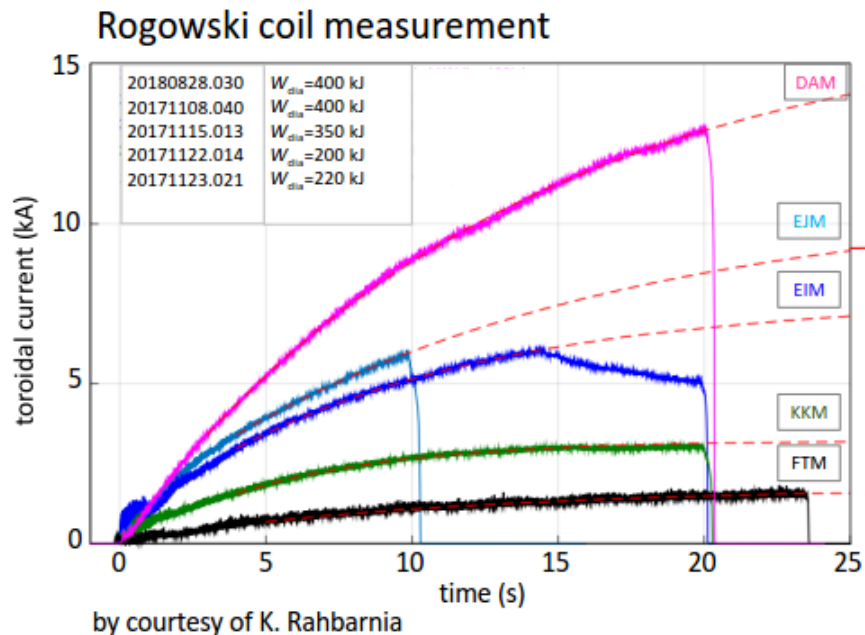
Bootstrap current minimization (limiter plasma)

- Two nearly identical plasmas in \sqrt{v} -regime dominated by strong ambipolar E_r
- Essential differences: Mirror ratio, ε_{eff}
⇒ Different bootstrap currents
- Toroidal curvature & helical component of magnetic field were the same (different ε_{eff} does not play a role in the \sqrt{v} -regime)
⇒ Same neoclassical energy transport / heat fluxes
- Ratio of bootstrap currents (no current drive) match neoclassical predictions
- Bootstrap current minimization: Factor 3.5 smaller than in equivalent tokamak

A. Dinklage et al., A. Dinklage et al. (2018) Nature Physics
doi:10.1038/s41567-018-0141-9



Dependence of bootstrap current on magnetic field configuration



$$I(t) = I_{\text{BS}}(1 - e^{-(t-t_0)/\tau})$$

bootstrap current

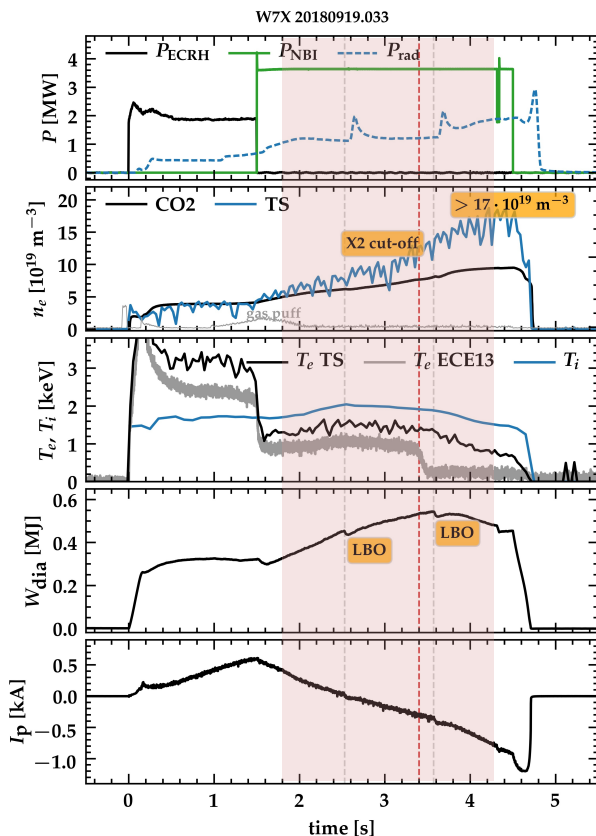
shielding current

good agreement with transport simulation
 but current offset due to ECCD contribution?

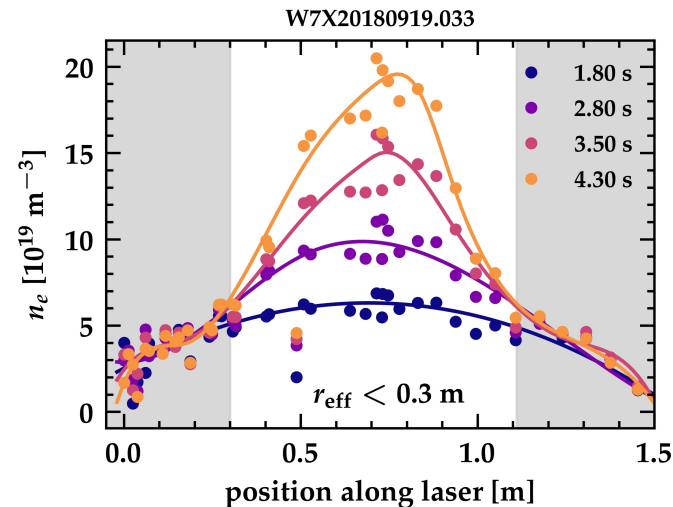


Extra Slides

Pure NBI heating changes (particle) transport

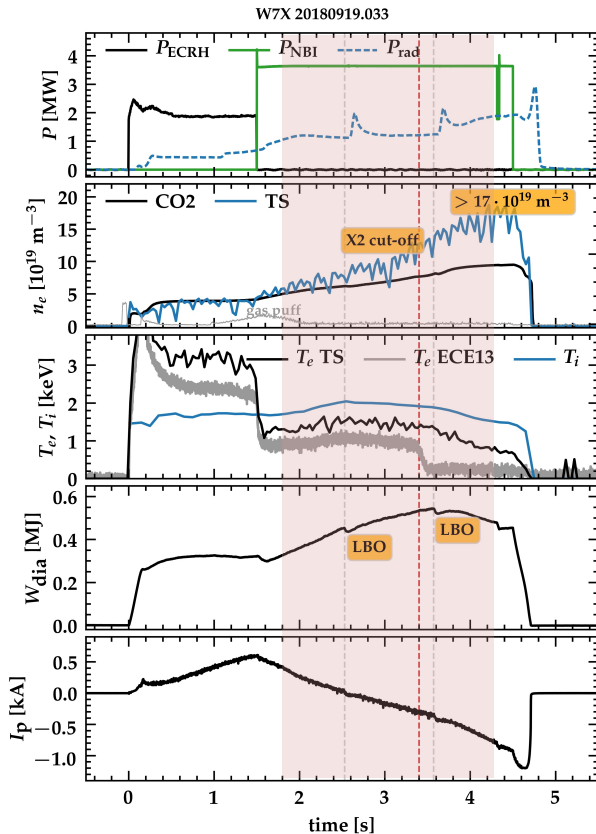


n_e
(Thomson scattering)

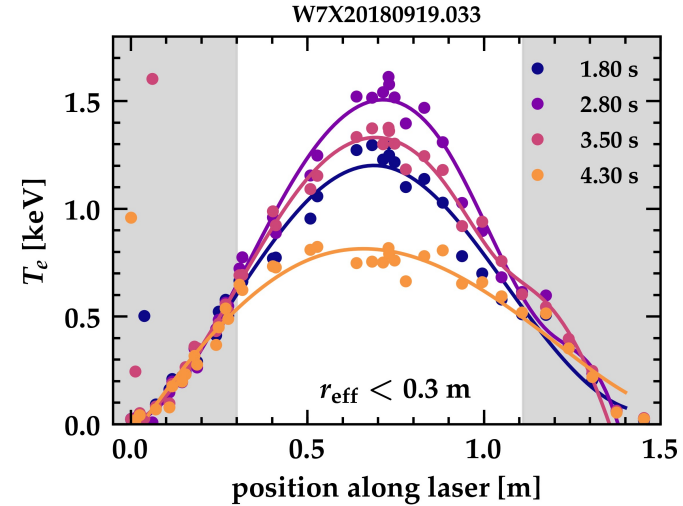


- Plasma can be sustained by pure NBI heating
- Centrally peaked high density plasma develops
- Density peaking can be controlled with ECRH
- Pure NBI heating with $n_{e0} = 2 \times 10^{20} \text{ m}^{-3}$ demonstrated

Pure NBI heating changes (particle) transport



T_e
(Thomson scattering)



- Plasma can be sustained by pure NBI heating
- Centrally peaked high density plasma develops
- Density peaking can be controlled with ECRH
- Pure NBI heating with $n_{e0} = 2 \times 10^{20} \text{ m}^{-3}$ demonstrated

MEASURED RADIAL ELECTRIC FIELD AT W7X PROVIDES CONFIDENCE IN NEOCLASSICAL CALCULATIONS

The ambipolar radial electric field can be predicted from the measured T_e , T_i and n_e profiles.

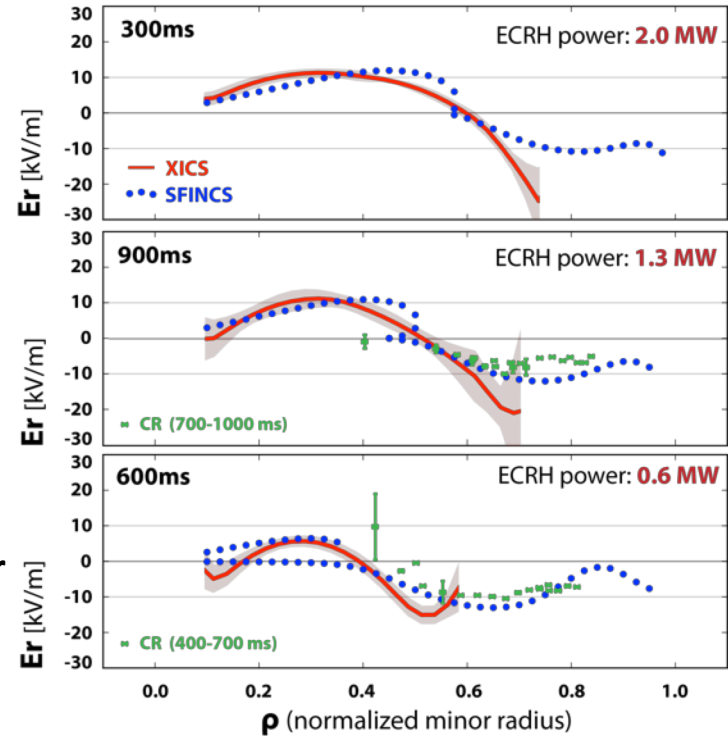
Neoclassical calculations by the SFINCS code:

- **SFINCS:** 4D Drift-Kinetic continuum code. Includes compressible ExB drift.

Neoclassical predictions for E_r show similar structure and magnitude to measured profiles.

- **Crossover** from electron-root to ion-root in **excellent agreement.**

Measurements of E_r from the Correlation Reflectometer agree well with neoclassical in the outer portion of the plasma.



VALIDATION AND CROSS COMPARISON OF NEOCLASSICAL TRANSPORT CALCULATIONS IN STELLARATORS

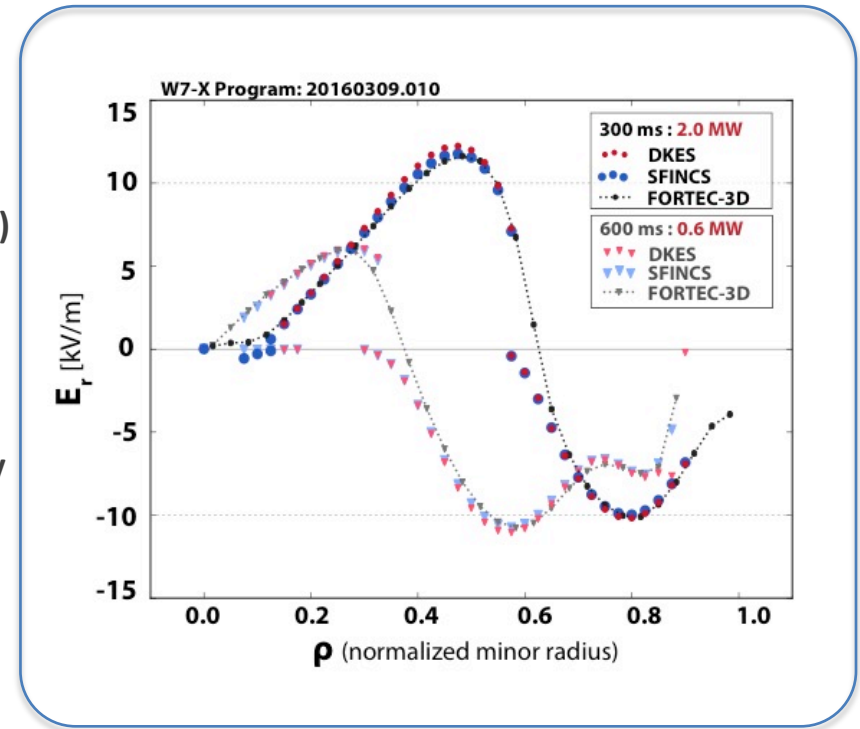
State of the art codes for calculation of neoclassical transport has been validated and compared at both W7-X and LHD.

- **FORTEC-3D** S. Satake (NIFS)
- **SFINCS** M. Landreman (University of Maryland)
- **DKES** W. van Rij (ORNL)

Comparison to measured radial electric fields provides **experimental validation of the code results.**

Comparisons between codes allows regimes of code validity to be studied.

These results represent the first experimental validation and cross-comparison of neoclassical transport calculations on W7-X!



INITIAL INVESTIGATIONS ON THE ROLE OF OF NEOCLASSICAL TRANSPORT IN W7-X PLASMAS HAVE BEGUN

Neoclassically the majority of heat is lost through the electron channel.

- Expected due to weak coupling between electrons and ions at low densities.

At high power the maximum neoclassical transport in the core is about 50% of the input heating power.

- Turbulence and radiation losses are expected to dominate in the edge.

Likely candidates to explain the remaining heat transport or heat loss:

- Turbulent transport
- radiation losses
- charge exchange losses

